universität wien

MASTERARBEIT / MASTER'S THESIS

Titel der Masterarbeit / Title of the Master's Thesis

„Mathematical modeling and numerics of particle-laden flows: unresolved CFD-DEM“

verfasst von / submitted by

Roman Kostal, B.Sc.

angestrebter akademischer Grad / in partial fulfilment of the requirements for the degree of

Master of Science (MSc)

Wien, 2023 / Vienna, 2023

Studienkennzahl lt. Studienblatt / degree programme code as it appears on the student record sheet:	UA 066 821
Studienrichtung lt. Studienblatt / degree programme as it appears on the student record sheet:	Masterstudium Mathematik
Betreut von / Supervisor:	Univ.-Prof. Dr. Norbert Mauser

Abstract

The problem of simultaneous flow of a fluid and a granular material is one of large interest to natural scientists and engineers alike. In this thesis we deal with the mathematical modeling and numerics for this problem. Recent advances in computing allow tracking large numbers of particles in a Lagrangian manner by the so-called discrete element method (DEM), while solving for the fluid flow field by standard methods of computational fluid dynamics (CFD). After briefly discussing various approaches to this problem, we look in detail at the so-called unresolved CFD-DEM paradigm, which employs a volume-averaged version of the Navier-Stokes equations (VANS). We derive the VANS equations by using the theory of distributions as introduced by Schwartz and then examine how the VANS equations are coupled to particle calculations when obtaining a numerical solution. Finally, we compare some methods for calculating the volume fraction.

Zusammenfassung

Das Problem der gleichzeitigen Strömung einer Flüssigkeit und eines körnigen Materials ist für Naturwissenschaftler:innen und Ingenieur:innen gleichermaßen von großem Interesse. In dieser Arbeit beschäftigen wir uns mit der mathematischen Modellierung und Numerik für dieses Problem. Fortschritte in der Computertechnik ermöglichen es, eine große Anzahl von Partikeln mit der so genannten Diskrete-Elemente-Methode (DEM) zu verfolgen, während das Strömungsfeld mit Standardmethoden der numerischen Strömungsmechanik (CFD) gelöst wird. Nach einer kurzen Besprechung verschiedener Ansätze für dieses Problem befassen wir uns ausführlich mit dem so genannten unaufgelösten CFD-DEM-Paradigma, bei dem eine volumengemittelte Version der Navier-Stokes-Gleichungen (VANS) verwendet wird. Wir leiten die VANS-Gleichungen mit Hilfe der von Schwartz eingeführten Verteilungstheorie her und untersuchen dann, wie die VANS-Gleichungen bei der numerischen Lösung mit Partikelberechnungen gekoppelt werden. Schließlich vergleichen wir einige Methoden zur Berechnung des Volumenanteils.

Table of contents

List of figures

1. Introduction

1.1. Real-world problems, motivation

The simultaneous flow of a fluid and a granular material occurs abundantly in the natural world. When solving related problems, one of the two phases can usually be ignored due to its negligible influence on the other phase and because there is no interest in information about this phase. As an example, consider the flow of water in the oceans and rivers. A sample of the water will contain many small pieces of deformable as well as non-deformable solids but these are not taken into account when calculating e.g. the height of a water wave. In other situations both phases must be taken into account and predicting their motions can be of high interest. Examples from the natural world include sediment transport, flow of liquid water with pieces of ice, flow of lava with pieces of rock and many others. Those from the world of engineering include fluidized-bed reactors, pneumatic conveying systems and dryers. To give a concrete example, consider *counter-current rotary drum dryers*, used to dry anything from gravel to harvested crops. Displayed in figure 1.1, this simple piece of equipment consists of a slightly tilted cylindrical chamber rotating with an angular velocity ω where a mass flow of granular solids $\dot{m}_s$ with temperature T_s and moisture content Q_s enters on one end and is carried by gravity towards the other end. Here, a hot gas is blown into the chamber to heat up the solids, foster evaporation, and advect the evaporated moisture out of the system. To increase the surface area over which heat and mass transfer take place, the granular material is lifted from the bottom of the drum by protrusions in the walls, so called *flights*, and then falls back down continuously while moving through the upper section.

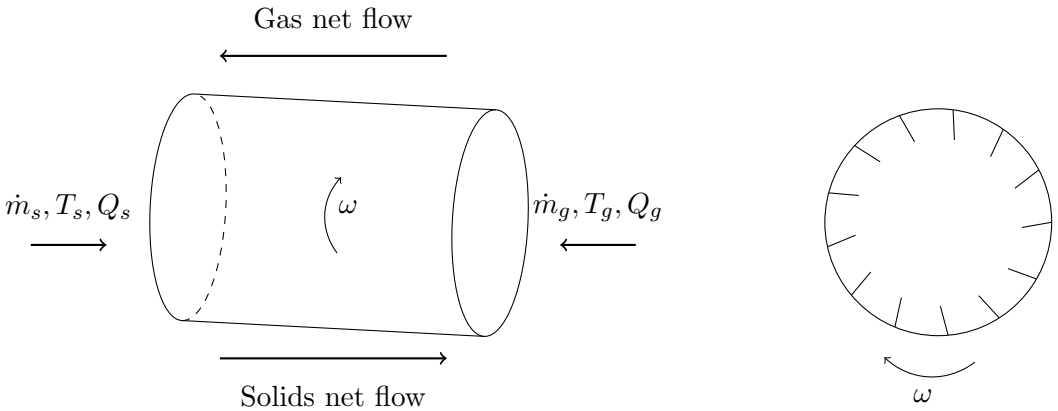

Figure 1.1.: Schematic of a rotary drum dyer

1.2. Approaches to modeling particle-fluid flows

There is a growing interest in simulating these systems to optimize their design, predict the effects of new drying media, geometric configurations, etc., and a variety of ways of doing so. A literature review reveals a rich palette of models which can be divided into two categories:

- Eulerian-Eulerian models, which model both the fluid and the particles as interpenetrating continua occupying a common region of space. Originally developed for the problem of two immiscible fluids [1] [2], the model can accommodate an arbitrary number of phases, where each phase obeys its own pair of fluid-like continuity and momentum equations. A recent example application to a rotating drum problem is the work of Delele et.al. [3]. We state a version with a single fluid phase and a single solid phase to illustrate:

$$\begin{aligned}
&\frac{\partial}{\partial t}\left(\alpha_f \rho_f\right) + \operatorname{div}\left(\alpha_f \rho_f \overline{\mathbf{v}}_f\right) = 0 \\
&\frac{\partial}{\partial t}\left(\alpha_f \rho_f \overline{\mathbf{v}}_f\right) + \operatorname{div}\left(\alpha_f \rho_f \overline{\mathbf{v}}_f \otimes \overline{\mathbf{v}}_f\right) = \operatorname{div} \mathbf{T}_f + \alpha_f \rho_f \mathbf{g} - \mathbf{F}_{fs} \\
&\frac{\partial}{\partial t}\left(\alpha_s \rho_s\right) + \operatorname{div}\left(\alpha_s \rho_s \overline{\mathbf{v}}_s\right) = 0 \\
&\frac{\partial}{\partial t}\left(\alpha_s \rho_s \overline{\mathbf{v}}_s\right) + \operatorname{div}\left(\alpha_s \rho_s \overline{\mathbf{v}}_s \otimes \overline{\mathbf{v}}_s\right) = \operatorname{div} \mathbf{T}_s + \alpha_s \rho_s \mathbf{g} + \mathbf{F}_{fs}
\end{aligned} \tag{1.1}$$

  Where the subscripts f and s are used to label the variables representing the fluid and the solid phase and α is the local volume fraction of each phase such that $\alpha_f + \alpha_s = 1$. All functions in this equation except for the gravitational acceleration vector $\mathbf{g}$ are local averages and are defined throughout the domain of interest. This is in contrast to the *primitive functions* such as the fluid velocity $\mathbf{v}_f$, which is defined only at the points occupied by the fluid at a given point in space and time. The advantage of this model is that the equations (1.1) can be discretized and solved by any of the well developed numerical methods of computational fluid dynamics (CFD). The main difficulty consists of providing an expression for $\mathbf{T}_s$ and $\mathbf{F}_{fs}$. While the form of the stress tensor $\mathbf{T}_f$ is well known for various types of fluids, there is no universally accepted analog for the solid phase.

- Eulerian-Lagrangian models, where the solid phase is treated at the level of individual particles, whose positions, momenta and angular momenta are tracked in a Lagrangian manner by numerically solving the equations of motion of classical mechanics, while also resolving all the collisions among the particles. This is accomoplished by the so-called discrete element method (DEM).
  For the fluid phase, a pair of continuity and momentum equations are solved. The natural question which arises in this context is that of the fluid domain: since the coordinates of the particles at each time-step are the output of the DEM solver, the region of space Φ occupied by the fluid is also known. However, Φ is time-dependent

and to solve the fluid equations on Φ by a chosen CFD method requires a *moving computational mesh*. This approach, referred to as *resolved* CFD-DEM, in principle resolves the flow around the particles but is computationally very expensive. Hager et. al. [4] report applicability of this method to cases involving up to about 10^3 particles. Problems of scientific or engineering interest typically involve 10^7 or more particles and furthermore, their diameter is often two orders of magnitude smaller than the typical fluid velocities involved. Since the mesh cells must be even smaller than the particles to get any hope of resolving the flow around them, satisfying a CFL condition

$$C := \Delta t \left(\sum_{i=1}^{n} \frac{v_i}{\Delta x_i} \right) \leq C_{\max}$$

then usually requires a prohibitively small Δt.
Hence, in these situation another approach is chosen: instead of tracking the fluid region in time by a moving mesh and solving the fluid equations on it, an averaged version of the equations is solved on a fixed mesh which spans the entire domain of interest, just like in the Eulerian-Eulerian approach. The presence of the particles then enters the fluid equations both as a scalar field representing the fraction of volume occupied by the particles locally, and as a source term in the momentum equation representing the momentum exchange between the particles and the fluid. This enables the use of a well validated model for each of the phases, at a reasonable computational cost. In the next two chapters we will, inspired by the work of Drew [2], who used distributions in his Eulerian-Eulerian model, aim to derive the volume averaged Navier-Stokes equations (VANS) for a single incompressible fluid phase mixed with a single granular solid phase.

Figure 1.2.: A side by side comparison of example meshes used for resolved (upper half) and unresolved (lower half) CFD-DEM

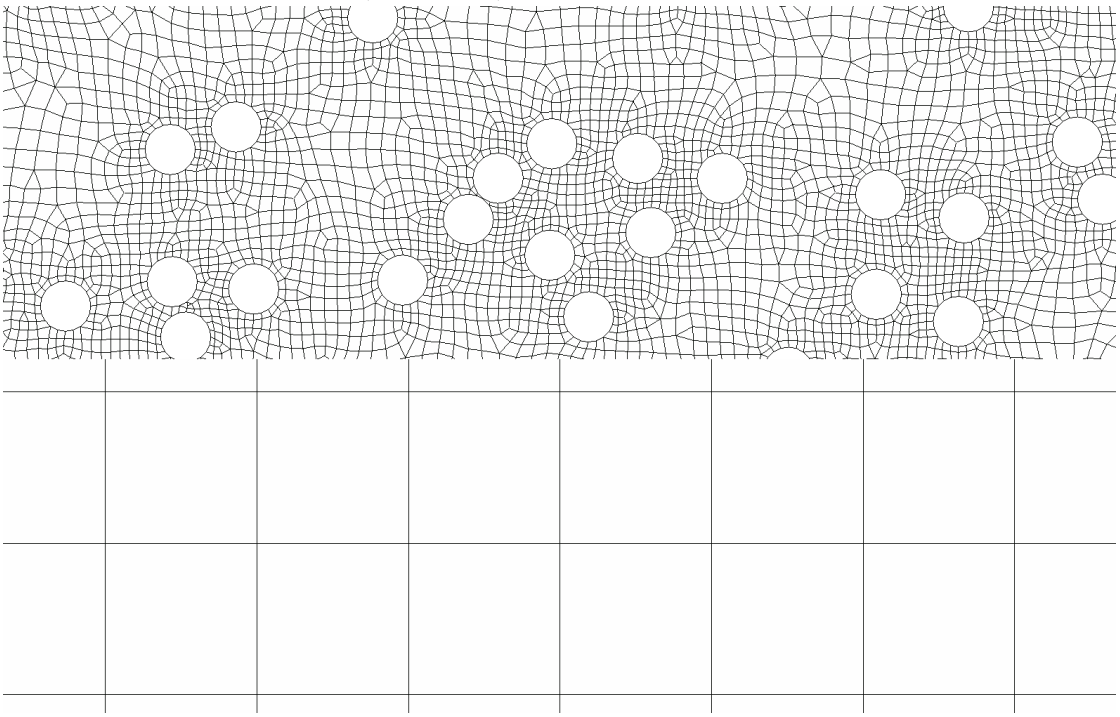

2. Preliminaries

In this chapter, we setup the framework and working tools which will be used in deriving a the VANS equations for a mixed granular-fluid flow.

2.1. Domain and boundary conditions

The domain of interest Ω consists of two disjoint subsets: the fluid phase $\Phi \subset \mathbb{R}^3$ and the solid phase $\Sigma \subset \mathbb{R}^3$. The solid phase consists of a finite number $N_p \in \mathbb{N}$ of individual particles $P_i \subset \mathbb{R}^3$. The P_i are bounded with a piecewise smooth boundary, simply connected, convex and such that:

$$\Sigma = \bigcup_{i=1}^{N_p} P_i$$

$$P_i \cap P_j = \emptyset \text{ for } i \neq j.$$

We further define the boundary of the solid phase $\partial\Sigma$ as follows:

$$\partial\Sigma = \bigcup_{i=1}^{N_p} \partial P_i$$

where ∂P_i is the boundary of P_i. By construction, $\partial\Sigma$ is piecewise smooth. We will assume that at all times, $\Phi \cup \Sigma = \Omega = \mathbb{R}^3$.
It is useful to define the indicator functions of the fluid and solid phases by

$$\chi_f(\mathbf{x}, t) := \begin{cases} 1 & \text{if } \mathbf{x} \in \Phi \\ 0 & \text{if } \mathbf{x} \notin \Phi \end{cases}$$

$$\chi_s(\mathbf{x}, t) := \begin{cases} 1 & \text{if } \mathbf{x} \in \Sigma \\ 0 & \text{if } \mathbf{x} \notin \Sigma \end{cases}.$$

We assume that there exists a smooth velocity field $\mathbf{v}(\mathbf{x}, t) : \mathbb{R}^3 \times \mathbb{R} \to \mathbb{R}^3$, giving the velocity at each point $(\mathbf{x}, t)$, irrespective of whether $(\mathbf{x}, t)$ belongs to the fluid phase or the solid phase.

Assumption 1. *(No-slip boundary condition) For every sequence of points $\{\mathbf{x}_j\} \subset \Phi$, such that*

$$\lim_{j\to\infty} \mathbf{x}_j = \mathbf{x}_{lim} \in \partial\Sigma,$$

we have

$$\lim_{j\to\infty} \mathbf{v}(\mathbf{x}_j) = \mathbf{v}(\mathbf{x}_{lim})$$

2.2. Properties of distributions

This section is based on the classical works of Schwartz [5] and Treves [6].
The indicator function is obviously not differentiable, but it is locally integrable ($\chi(\mathbf{x},t) \in L^1_{loc}(\mathbb{R}^3 \times \mathbb{R})$), meaning for every compact set $K \in \mathbb{R}^3 \times \mathbb{R}$

$$\int_K |\chi(\mathbf{x},t)|\, d\mathbf{x}dt < \infty.$$

This means that we can, for example, look at the average velocity of the fluid in a compact subset $K \subset \mathbb{R}^3$ by evaluating

$$\int_K \chi(\mathbf{x},t)\mathbf{v}(\mathbf{x},t)\, d\mathbf{x}dt$$

Definition 1 (Test function)**.** *On an open subset $\Omega \subset \mathbb{R}^n$, the vector space $\mathcal{D}(\Omega)$ of test functions $\varphi(\mathbf{x})$ consists of functions posessing an arbitrary number of continuous partial derivatives and such that* $\operatorname{supp}(\varphi)$ *is bounded and does not intersect the boundary of Ω.*

Definition 2 (Distribution)**.** *A continuous linear functional on the vector space $\mathcal{D}(\Omega)$ is called a distribution.*

Based on these definitions we show that χ defines a distribution T_χ on $C_c^\infty(\mathbb{R}^3 \times \mathbb{R}$ as follows:

$$\langle T_\chi, \varphi\rangle := \int_{\mathbb{R}^3\times\mathbb{R}} \chi(\mathbf{x})\varphi(\mathbf{x})\, d\mathbf{x}dt, \quad \varphi \in C_c^\infty(\mathbb{R}^3 \times \mathbb{R}). \tag{2.1}$$

The integral is finite since the domain of integration is restricted to the support of φ where φ is continuous and χ integrable so $\chi\varphi$ is integrable. Linearity follows form the linearity of integration. Regarding continuity, let $\varphi_j \to \varphi$ in $\mathcal{D}$ and let K be the bounded set contatining the supports of all the φ_j. Then

$$|\langle T_\chi, \varphi_j\rangle - \langle T_\chi, \varphi\rangle| \leq \left(\int_K \chi(\mathbf{x})\, d\mathbf{x}dt\right) \max\left(|\varphi(\mathbf{x})_j - \varphi(\mathbf{x})|\right) \to 0. \tag{2.2}$$

A *regular disribution* is one which we can define as we defined T_χ, by integrating. A useful fact about regular distributions is the content of the following theorem.

Theorem 1. *Two locally integrable functions χ and ξ define the same distribution $T_\chi = T_\xi$ if and only if χ and ξ are equal up to a set of measure zero.*

Proof. If χ and ξ are equal almost everywhere, 2.1 gives the same result for both functions, so they obviously define the same distribution. For proof of the reverse see Schwartz [5] page 74. Theorem 2. □

Another example of a distribution, this time not regular, is the δ_a defined by

$$\langle \delta_a, \varphi \rangle := \varphi(a), \quad \varphi \in \mathcal{D}(\Omega).$$

The linearity and continuity of δ_a is trivial.

Definition 3. *Let T be a distribution on $\mathcal{D}(\Omega)$. Then the derivative of T with respect to x_i is the distribution $\frac{\partial T}{\partial x_i}$ defined as follows:*

$$\left\langle \frac{\partial T}{\partial x_i}, \varphi \right\rangle = - \left\langle T, \frac{\partial \varphi}{\partial x_i} \right\rangle$$

One quickly checks that this is a valid definition of a distribution. For the second derivative we then have:

$$\left\langle \frac{\partial^2 T}{\partial x_i \partial x_j}, \varphi \right\rangle = - \left\langle \frac{\partial T}{\partial x_j}, \frac{\partial \varphi}{\partial x_i} \right\rangle = \left\langle T, \frac{\partial^2 \varphi}{\partial x_j \partial x_i} \right\rangle$$
$$\left\langle \frac{\partial^2 T}{\partial x_j \partial x_i}, \varphi \right\rangle = - \left\langle \frac{\partial T}{\partial x_i}, \frac{\partial \varphi}{\partial x_j} \right\rangle = \left\langle T, \frac{\partial^2 \varphi}{\partial x_i \partial x_j} \right\rangle$$

By the continuity of the second derivatives of φ it follows that

$$\frac{\partial^2 T}{\partial x_i \partial x_j} = \frac{\partial^2 T}{\partial x_j \partial x_i}.$$

and thus for any multiindex $p = (p_1, \ldots, p_n)$, $p_i \in \mathbb{N}$ with $|p| = \sum_{i=1}^n p_i$ we have

$$\langle \mathrm{D}^p_{\mathbf{x}} T, \varphi \rangle = -1^{|p|} \langle T, \mathrm{D}^p_{\mathbf{x}} \varphi \rangle$$

where $\mathrm{D}^p_{\mathbf{x}} = \left(\frac{\partial}{\partial x_1}\right)^{p_1} \left(\frac{\partial}{\partial x_2}\right)^{p_2} \ldots \left(\frac{\partial}{\partial x_n}\right)^{p_n}$.

Theorem 2 (Schwartz 1966 [5], page 91, Theorem 7)**.** *If T is an arbitrary distribution and f a $C^\infty(\Omega)$ function, then the product fT defines a distribution in the following way:*

$$\langle fT, \varphi \rangle = \langle T, f\varphi \rangle$$

We demonstrate the use of the definitions and Theorem 2 by way of example: consider the distribution $\mathbf{v} \cdot \nabla \chi_f$ and its action on a test function φ:

$$\langle \mathbf{v} \cdot \nabla \chi_f, \varphi \rangle = \left\langle \sum_{j=1}^{3} v_j \frac{\partial \chi_f}{\partial x_j}, \varphi \right\rangle \tag{2.3}$$

$$= \sum_{j=1}^{3} \left\langle v_j \frac{\partial \chi_f}{\partial x_j}, \varphi \right\rangle \tag{2.4}$$

$$= \sum_{j=1}^{3} \left\langle \frac{\partial \chi_f}{\partial x_j}, v_j \varphi \right\rangle \tag{2.5}$$

$$= -\sum_{j=1}^{3} \left\langle \chi_f, \frac{\partial (v_j \varphi)}{\partial x_j} \right\rangle \tag{2.6}$$

$$= -\left\langle \chi_f, \sum_{j=1}^{3} \left(\frac{\partial v_j}{\partial x_j} \varphi + \frac{\partial \varphi}{\partial x_j} v_j \right) \right\rangle \tag{2.7}$$

$$= -\langle \chi_f, (\operatorname{div} \mathbf{v})\, \varphi + \mathbf{v} \cdot \nabla \varphi \rangle = -\langle \chi_f, \operatorname{div}(\mathbf{v}\varphi) \rangle \tag{2.8}$$

We will also make frequent use of the product rule:

Theorem 3 (Schwartz 1966 [5], page 93, Theorem 9)**.** *For a smooth function f and a distriution T, the product rule for derivatives holds:*

$$\frac{\partial}{\partial x_i}(fT) = \frac{\partial f}{\partial x_i} T + f \frac{\partial T}{\partial x_i}.$$

Proof. We evaluate all three distributions from the above eqation on a test function φ:

$$\left\langle \frac{\partial}{\partial x_i}(fT), \varphi \right\rangle = -\left\langle fT, \frac{\partial \varphi}{\partial x_i} \right\rangle = -\left\langle T, f \frac{\partial \varphi}{\partial x_i} \right\rangle,$$
$$\left\langle \frac{\partial f}{\partial x_i} T, \varphi \right\rangle = \left\langle T, \frac{\partial f}{\partial x_i} \varphi \right\rangle,$$
$$\left\langle f \frac{\partial T}{\partial x_i}, \varphi \right\rangle = \left\langle \frac{\partial T}{\partial x_i}, f\varphi \right\rangle = -\left\langle T, \frac{\partial}{\partial x_i}(f\varphi) \right\rangle.$$

Adding the second and third lines and using bilinearity, the proof reduces to showing that

$$-f \frac{\partial \varphi}{\partial x_i} = \frac{\partial f}{\partial x_i} \varphi - \frac{\partial}{\partial x_i}(f\varphi)$$

which is just the product rule for ordinary functions. □

We now apply the product rule to show a result that will be used several times in what follows. Consider an arbitrary point $(\mathbf{x}, t)$. This point either belongs to the fluid phase or the solid phase. It is intuitively clear that if we follow the material element which was

at the location $\mathbf{x}$ at the time t on its trajectory, it will forever be a member of the same phase. To make this precise, we show that the convective derivative of $\chi_f(\mathbf{x}, t)$ is zero:

$$\frac{\partial \chi_f}{\partial t} + \mathbf{v} \cdot \nabla \chi_f = 0 \tag{2.9}$$

in the sense of distributions.
To see this, consider

$$\left\langle \frac{\partial \chi_f}{\partial t} + \mathbf{v} \cdot \nabla \chi_f, \varphi \right\rangle = -\left\langle \chi_f, \frac{\partial \varphi}{\partial t} + \operatorname{div}(\varphi \mathbf{v}) \right\rangle \tag{2.10}$$

$$= -\int_{\mathbb{R}^3 \times \mathbb{R}} \chi_f \left(\frac{\partial \varphi}{\partial t} + \operatorname{div}(\varphi \mathbf{v}) \right) d\mathbf{x} dt \tag{2.11}$$

$$= -\int_{-\infty}^{\infty} \left(\int_{\Phi(t)} \left(\frac{\partial \varphi}{\partial t} + \operatorname{div}(\varphi \mathbf{v}) \right) d\mathbf{x} \right) dt \tag{2.12}$$

$$= -\int_{-\infty}^{\infty} \left(\frac{d}{dt} \int_{\Phi(t)} \varphi \, d\mathbf{x} \right) dt \tag{2.13}$$

$$= -\int_{\Phi(t)} \varphi \, d\mathbf{x} \Big|_{-\infty}^{\infty} = 0. \tag{2.14}$$

Here (2.10) is the definition of the derivative and (2.12) holds by definition of χ_f. To get to (2.13) we apply the Reynolds transport theorem, see appendix (B.11). (2.14) is the fundamental theorem of calculus and compact support of φ.

The last tool we will need is the convolution.

Theorem 4 (Convolution, Trèves [6], page 287, theorem 27.2)**.** *Let φ be a C^∞ function, and T a distribution in $\mathbb{R}^n$. Suppose that at least one of the two sets,* $\operatorname{supp}(\varphi), \operatorname{supp}(T)$, *is compact. Then*

$$\mathbf{x} \mapsto \langle T, \varphi(\mathbf{x} - \mathbf{y}) \rangle$$

is a C^∞ function in $\mathbb{R}^n$. For any mutltiindex $p = (p_1, \ldots, p_n)$, we have

$$\mathrm{D}^p_{\mathbf{x}} \langle T(\mathbf{y}), \varphi(\mathbf{x} - \mathbf{y}) \rangle = \langle T(\mathbf{y}), \mathrm{D}^p_{\mathbf{x}} \varphi(\mathbf{x} - \mathbf{y}) \rangle .$$

Where we have introduced the (abuse of) notation $T(\mathbf{y})$ to indicate that the distribution T acts on a function $\varphi(\mathbf{x} - \mathbf{y})$ when the latter is regarded as a function of $\mathbf{y}$.

Furthermore, we note that

$$\begin{aligned} \langle T(\mathbf{y}), \mathrm{D}^p_{\mathbf{x}} \varphi(\mathbf{x} - \mathbf{y}) \rangle &= \left\langle T(\mathbf{y}), (-1)^{|p|} \mathrm{D}^p_{\mathbf{y}} \varphi(\mathbf{x} - \mathbf{y}) \right\rangle \\ &= \left\langle \mathrm{D}^p_{\mathbf{y}} T(\mathbf{y}), \varphi(\mathbf{x} - \mathbf{y}) \right\rangle \end{aligned}$$

So that we also have

$$\left\langle \mathrm{D}_{\mathbf{y}}^{p} T(\mathbf{y}), \varphi(\mathbf{x}-\mathbf{y}) \right\rangle = \mathrm{D}_{\mathbf{x}}^{p} \left\langle T(\mathbf{y}), \varphi(\mathbf{x}-\mathbf{y}) \right\rangle \tag{2.15}$$

just like for convolution of ordinary functions.

Definition 4 (Convolution)**.** *The function* $T * \varphi : \mathbb{R}^n \to \mathbb{R}^n$

$$\mathbf{x} \mapsto \langle T(\mathbf{y}), \varphi(\mathbf{x}-\mathbf{y}) \rangle$$

is called the convolution of φ *and* T *and denoted by* $T * \varphi$ *or* $\varphi * T$*. When the distribution* T *is regular, we have*

$$\langle T_f(\mathbf{y}), \varphi(\mathbf{x}-\mathbf{y}) \rangle = \int_{\mathbb{R}^n} f(\mathbf{y}) \varphi(\mathbf{x}-\mathbf{y}) \, d\mathbf{y}.$$

2.3. Volume averaging

As stated in the introduction, our goal is to derive a version of the fluid equations written in terms of functions which, for a given $\mathbf{x} \in \mathbb{R}^3$ give an average of a quantity in a small region around $\mathbf{x}$ and such that they are differentiable $\mathbf{x} \in \mathbb{R}^3$. A standard tool in PDE theory used to achieve this is to convolve the nonsmooth function with a *mollifier*.

Definition 5 (Mollifier, Evans [7])**.** *Define* $\eta \in C_c^\infty(\mathbb{R}^n)$ *by*

$$\eta(\mathbf{x}) := \begin{cases} C \exp\left(\frac{1}{\|\mathbf{x}\|^2 - 1}\right) & \text{if } \|\mathbf{x}\| < 1 \\ 0 & \text{if } \|\mathbf{x}\| \geq 1, \end{cases}$$

the constant $C > 0$ *selected so that* $\int_{\mathbb{R}^n} \eta \, d\mathbf{x} = 1$*. For each* $\epsilon > 0$*, set*

$$\eta_\epsilon(\mathbf{x}) := \frac{1}{\epsilon^n} \eta\left(\frac{\mathbf{x}}{\epsilon}\right).$$

We call η *the standard mollifier. The functions* η_ϵ *are* C^∞ *and satisfy*

$$\int_{\mathbb{R}^n} \eta_\epsilon \, d\mathbf{x} = 1, \qquad \operatorname{supp}(\eta_\epsilon) \subset B(0, \epsilon).$$

In addition to *smoothing*, the mollifier of choice should also perform *filtering* and *weighing*. That is, ϵ needs to be chosen such that it filters out features which are irrelevant to the problem. For example, if the particles have diameter d, we might choose $\epsilon = 3d$. We will call this η_ϵ the weight function.

Definition 6. *The weighted space average (WSA) of a locally integrable function* ϕ *is defined as its convolution of* $\phi \chi_f$ *with the weight function:*

$$\widetilde{\phi}(\mathbf{x}, t) := (\chi_f \phi) * w = \int_\Omega \chi_f(\mathbf{y}, t) \phi(\mathbf{y}, t) w(\mathbf{x}-\mathbf{y}) \, d\mathbf{y}. \tag{2.16}$$

Definition 7. *The local volume fraction of the fluid phase α_f is given by*

$$\alpha_f(\mathbf{x},t) = \chi_f * w = \int_\Omega \chi_f(\mathbf{y},t) w(\mathbf{x}-\mathbf{y})\ d\mathbf{y} \tag{2.17}$$

Definition 8. *The weighted phasic average (WPA) in the fluid phase of a locally integrable function ϕ is defined as:*

$$\overline{\phi}(\mathbf{x},t) = \frac{(\chi_f \phi) * w}{\alpha_f(\mathbf{x},t)} = \frac{\int_\Omega \chi_f(\mathbf{y},t)\phi(\mathbf{y},t) w(\mathbf{x}-\mathbf{y})\ d\mathbf{y}}{\int_\Omega \chi_f(\mathbf{y},t) w(\mathbf{x}-\mathbf{y})\ d\mathbf{y}} \tag{2.18}$$

We see that the WPA of ϕ is just the WSA of ϕ scaled appropriately. Indeed, a useful average should satisfy, for $c \in \mathbb{R}$

$$\overline{c} = c,$$

which is the case for the WPA. For the WSA, we have

$$\widetilde{c} = \alpha_f c,$$

Properties of the WSA

We list five useful properties of the WSA, which hold for arbitrary $f, g \in L^1_{loc}(\mathbb{R}^3)$ and $c \in \mathbb{R}$:

1. $\widetilde{f+g} = \widetilde{f} + \widetilde{g}$
2. $\widetilde{cf} = c\widetilde{f}$
3. $\widetilde{fg} \neq \widetilde{f}\widetilde{g}$
4. $\widetilde{\dfrac{\partial f}{\partial x_i}} = \dfrac{\partial}{\partial x_i}\widetilde{f}$
5. $\widetilde{\dfrac{\partial f}{\partial t}} = \dfrac{\partial}{\partial t}\widetilde{f}$

Items 1., 2. and 3. are familiar rules of integration. Property 4. follows from Theorem 4 and property 5. is justified by the following theorem.

Theorem 5 (Differentiating under the integral sign [8])**.** *Let $\psi(t,\mathbf{y}) : \mathbb{R}^{n+1} \to \mathbb{R}$ be a function such that for each fixed t, the integral*

$$\Psi(t) = \int_{\mathbb{R}^n} \psi(t,\mathbf{y}) d\mathbf{y}$$

exists. Suppose that $\frac{\partial \psi}{\partial t}$ exists for almost all $\mathbf{y}$. If there exists $\epsilon > 0$ and an L-integrable function ϑ such that for all $s \neq t$,

$$|s-t| < \epsilon \Longrightarrow \left| \frac{\psi(s,\mathbf{y}) - \psi(t,\mathbf{y})}{s-t} \right| \leq \vartheta(\mathbf{y}),$$

then Ψ is differentiable, and its derivative is

$$\frac{d\Psi}{dt}(t) = \int_{\mathbb{R}^n} \frac{\partial \psi}{\partial t}(t, \mathbf{y}) d\mathbf{y}$$

Proof. We compute

$$\begin{aligned}\frac{d\Psi}{dt}(t) &= \lim_{h\to 0} \frac{\Psi(t+h) - \Psi(t)}{h} = \lim_{h\to 0} \int_{\mathbb{R}^n} \frac{\psi(t+h, \mathbf{y}) - \psi(t, \mathbf{y})}{h} d\mathbf{y} \\ &= \int_{\mathbb{R}^n} \lim_{h\to 0} \frac{\psi(t+h, \mathbf{y}) - \psi(t, \mathbf{y})}{h} d\mathbf{y} = \int_{\mathbb{R}^n} \frac{\partial \psi}{\partial t}(t, \mathbf{y}) d\mathbf{y}.\end{aligned}$$

The third equality is justified by the dominated convergence theorem. □

Properties of the WPA

For the WPA, it follows from $\overline{f} = \dfrac{\widetilde{f}}{\alpha_f}$ that we have the following properties for arbitrary $f, g \in L^1_{loc}(\mathbb{R}^3)$ and $c \in \mathbb{R}$:

1. $\overline{f+g} = \overline{f} + \overline{g}$
2. $\overline{cf} = c\overline{f}$
3. $\overline{fg} \neq \overline{f}\,\overline{g}$
4. $\overline{\dfrac{\partial f}{\partial x_i}} \neq \dfrac{\partial}{\partial x_i}\overline{f}$
5. $\overline{\dfrac{\partial f}{\partial t}} \neq \dfrac{\partial}{\partial t}\overline{f}$

This is unfortunate, because it is the WPA that represents a meaningful average in terms of which the fluid equations should be written. The failure of the WPA to commute with derivatives will be a source of further complications in addition to ones arising from property 3.

3. Deriving the VANS equations

Assume that at each point $\mathbf{x}$ which belongs to the fluid phase at a particular time t, the incompressible Navier-Stokes system of equations[1] holds:

$$\operatorname{div} \mathbf{v} = 0 \tag{3.1}$$

$$\frac{\partial (\rho \mathbf{v})}{\partial t} + \operatorname{div} (\rho \mathbf{v} \otimes \mathbf{v}) = -\nabla p + \mu \Delta \mathbf{v} + \rho \mathbf{g}, \tag{3.2}$$

where μ and ρ are the fluid viscosity and density, respectively, p is the pressure and $\mathbf{g}$ is the gravitational acceleration vector and that the velocity and pressure fields are smooth. Our goal is to rewrite (3.1) and (3.2) in terms of $\overline{\mathbf{v}}$ and $\overline{p}$, which, by Theorem 4, are also smooth functions.

3.1. The continuity equation

Consider first the continuity equation

$$\operatorname{div} \mathbf{v} = 0, \tag{3.3}$$

which, in contrast to the momentum equation is also valid in the solid phase. The product with the indicator χ_f is the locally integrable function

$$\chi_f \operatorname{div} \mathbf{v} = 0$$

to which all of our previously introduced theory applies. In particular, by the product rule (Theorem 3), we have:

$$\chi_f \operatorname{div} \mathbf{v} = \operatorname{div}(\chi_f \mathbf{v}) - \nabla \chi_f \cdot \mathbf{v} \tag{3.4}$$

in the sense of distributions. Combining this with what we have shown in 2.9:

$$\nabla \chi_f \cdot \mathbf{v} = -\frac{\partial \chi_f}{\partial t},$$

we get that

$$\frac{\partial \chi_f}{\partial t} + \operatorname{div}(\chi_f \mathbf{v}) = 0. \tag{3.5}$$

[1] Of course, just 4.4 was derived by Navier and Stokes. However, 4.3 is always stated together with 4.4 to have four equations for four unknowns so we prefer to refer to the whole system as the Navier-Stokes equations, as do several other authors.

Now we convolve this distribution with our weight function of choice w and apply all the established rules:

$$\left(\frac{\partial \chi_f}{\partial t} + \operatorname{div}(\chi_f \mathbf{v})\right) * w = \frac{\partial \chi_f}{\partial t} * w + \operatorname{div}(\chi_f \mathbf{v}) * w \tag{3.6}$$

$$= \frac{\partial \left(\chi_f * w\right)}{\partial t} + \operatorname{div}(\chi_f \mathbf{v} * w) \tag{3.7}$$

$$= \frac{\partial \alpha_f}{\partial t} + \operatorname{div}(\alpha_f \overline{\mathbf{v}}) \tag{3.8}$$

Where the last equality is just the use of definitions 4.22 and 2.18. We have thus arrived at the continuity equation valid for the fluid phase:

$$\frac{\partial \alpha_f}{\partial t} + \operatorname{div}(\alpha_f \overline{\mathbf{v}}) = 0. \tag{3.9}$$

We note that this equation has the same form as the continuity equation for a compressible fluid. In particular, we now have

$$\operatorname{div} \overline{\mathbf{v}} = -\frac{1}{\alpha_f}\left(\overline{\mathbf{v}} \cdot \nabla \alpha_f + \frac{\partial \alpha_f}{\partial t}\right) \tag{3.10}$$

3.2. The momentum equation

Similarly, starting with the momentum equation,

$$\frac{\partial \left(\rho \mathbf{v}\right)}{\partial t} + \operatorname{div}\left(\rho \mathbf{v} \otimes \mathbf{v}\right) = -\nabla p + \mu \Delta \mathbf{v} + \rho \mathbf{g} \tag{3.11}$$

we multiply it by χ_f and establish some identities.

3.2.1. The transient and convective terms

Starting with the LHS, we rewrite the two terms using the product rule (Theorem 3):

$$\chi_f \frac{\partial \left(\rho \mathbf{v}\right)}{\partial t} = \frac{\partial (\chi_f \rho \mathbf{v})}{\partial t} - \rho \mathbf{v} \frac{\partial \chi_f}{\partial t} \tag{3.12}$$

$$\chi_f \operatorname{div}\left(\rho \mathbf{v} \otimes \mathbf{v}\right) = \operatorname{div}\left(\chi_f \rho \mathbf{v} \otimes \mathbf{v}\right) - \left(\rho \mathbf{v} \otimes \mathbf{v}\right) \cdot \nabla \chi_f, \tag{3.13}$$

and then use (2.9):

$$\frac{\partial \chi_f}{\partial t} = -\mathbf{v} \cdot \nabla \chi_f$$

in (3.12). Now we add 3.12 and 3.13 and see that:

$$\chi_f \frac{\partial (\rho \mathbf{v})}{\partial t} + \chi_f \operatorname{div} (\rho \mathbf{v} \otimes \mathbf{v}) = \frac{\partial (\chi_f \rho \mathbf{v})}{\partial t} + \operatorname{div} (\chi_f \rho \mathbf{v} \otimes \mathbf{v}) \tag{3.14}$$

The RHS of (3.14) is now ready to be convolved with a weight function of choice to fulfill the definition of the phasic average (2.18):

$$\left(\frac{\partial (\chi_f \rho \mathbf{v})}{\partial t} + \operatorname{div} (\chi_f \rho \mathbf{v} \otimes \mathbf{v}) \right) * w = \frac{\partial (\chi_f \rho \mathbf{v})}{\partial t} * w + \operatorname{div} (\chi_f \rho \mathbf{v} \otimes \mathbf{v}) * w \tag{3.15}$$

$$= \frac{\partial \left((\chi_f \rho \mathbf{v}) * w \right)}{\partial t} + \operatorname{div} \left((\chi_f \rho \mathbf{v} \otimes \mathbf{v}) * w \right) \tag{3.16}$$

$$= \frac{\partial \left(\rho \left((\chi_f \mathbf{v}) * w \right) \right)}{\partial t} + \operatorname{div} \left(\rho \left((\chi_f \mathbf{v} \otimes \mathbf{v}) * w \right) \right) \tag{3.17}$$

$$= \rho \frac{\partial}{\partial t} \left(\alpha_f \overline{\mathbf{v}} \right) + \rho \operatorname{div} \left(\alpha_f \overline{\mathbf{v} \otimes \mathbf{v}} \right) \tag{3.18}$$

Importantly, $\overline{\mathbf{v} \otimes \mathbf{v}} \neq \overline{\mathbf{v}} \otimes \overline{\mathbf{v}}$. To give an example, consider the 1-D case $v(x) = x$ and averages taken around zero. Then $\overline{v}(0)^2 = 0^2$ but $\overline{v^2}(0) = \overline{x^2}(0) > 0$.
So we make the ansatz:

$$\overline{\mathbf{v} \otimes \mathbf{v}} = \overline{\mathbf{v}} \otimes \overline{\mathbf{v}} + \mathcal{R}_c \tag{3.19}$$

where $\mathcal{R}_c$ denotes the residual stress from averaging the convective term.

3.2.2. The body force

Next we take a look at the RHS of (3.11), first multiplying it by χ_f:

$$\chi_f \left(-\nabla p + \mu \Delta \mathbf{v} + \rho \mathbf{g} \right) \tag{3.20}$$

Considering the terms inside the bracket from left to right, only the body force can be convolved in a straigtforward manner based on what we have already shown:

$$(\chi_f \rho \mathbf{g}) * w = \alpha_f \rho \overline{\mathbf{g}} = \alpha_f \rho \mathbf{g} \tag{3.21}$$

Terms one and two require some work because they contain differential operators. To arrive at phasic averages, we must again invoke the product rule.

3.2.3. The pressure term

We have:

$$-\chi_f \nabla p = -\nabla (\chi_f p) + p \nabla \chi_f. \tag{3.22}$$

Previously, the analogs of the second term of the RHS of 3.22 have combined with other terms to give zero. Here it is not the case and we have to evaluate the distribution $\nabla\chi_f$ explicitly. For $\varphi \in C_c^\infty(\mathbb{R}^3)$:

$$\begin{aligned}
\langle \nabla\chi_f, \varphi\rangle &= -\langle \chi_f, \nabla\varphi\rangle && (3.23)\\
&= -\int_{\mathbb{R}^3} \chi_f(\mathbf{x})\nabla\varphi(\mathbf{x})\, d\mathbf{x} && (3.24)\\
&= -\int_{\Phi(t)} \nabla\varphi(\mathbf{x})\, d\mathbf{x} && (3.25)\\
&= -\int_{\partial\Phi(t)} \varphi(\mathbf{x})\,\mathbf{n}\, dS && (3.26)
\end{aligned}$$

Where $\partial\Phi(t)$ is the boundary of the fluid phase and $\mathbf{n}$ is the unit normal vector pointing out of the fluid phase. The last equality follows from the divergence theorem.
Indeed, for an arbitrary constant vector $\mathbf{u}$, $\mathrm{div}(\mathbf{u}) = 0$ and $\mathbf{u}\cdot\nabla\varphi = \mathrm{div}(\varphi\mathbf{u})$ so that we can write:

$$\mathbf{u}\cdot\left(\int_{\Phi(t)} \nabla\varphi\, dV\right) = \int_{\Phi(t)} \nabla\cdot(\varphi\mathbf{u}) dV = \int_{\partial\Phi(t)} \varphi\mathbf{u}\cdot\mathbf{n}\, dS = \mathbf{u}\cdot\left(\int_{\partial\Phi(t)} \varphi\mathbf{n}\, dS\right)$$

Since the vector $\mathbf{u}$ was arbitrary, the integrals in the brackets are equal:

$$\int_{\Phi(t)} \nabla\varphi\, dV = \int_{\partial\Phi(t)} \varphi\mathbf{n}\, dS. \tag{3.27}$$

Returning to (3.23), and moving the minus sign next to $\mathbf{n}$ in (3.26), we have shown how the distribution $\nabla\chi_f$ acts on test functions: it picks out values of φ at the boundary of the fluid phase $\partial\Phi(t)$ and multiplies them by a unit vector pointing *into* the fluid phase and normal to the boundary. This is in agreement with the 1D situation, where the derivative of the Heaviside step is the delta distribution.

What does this mean for the averaging of the pressure term (3.22)?

$$\begin{aligned}
(-\chi_f\nabla p) * w &= -\nabla(\chi_f p) * w + (p\nabla\chi_f) * w && (3.28)\\
&= -\nabla((\chi_f p) * w) \underbrace{- \int_{\partial\Phi(t)} p(\mathbf{y}) w(\mathbf{x}-\mathbf{y})\mathbf{n}(\mathbf{y})\, dS}_{=:\,\hat{p}\hat{\mathbf{n}}|_{\partial\Phi}} && (3.29)\\
&= -\nabla\left(\alpha_f\overline{p}\right) + \hat{p}\hat{\mathbf{n}}|_{\partial\Phi} && (3.30)\\
&= -\alpha_f\nabla\overline{p} - \overline{p}\nabla\alpha_f + \hat{p}\hat{\mathbf{n}}|_{\partial\Phi} && (3.31)
\end{aligned}$$

We see that in addition to the gradient of the phase-averaged pressure $\alpha_f\nabla\overline{p}$, we get two more terms. The term $\hat{p}\hat{\mathbf{n}}|_{\partial\Phi}$ represents the weighted averaged pressure at the boundary in the direction of the fluid and is easy to interpret. It corresponds to the fact that when

the pressure is higher on one side of a solid body, there is a force on the body by the fluid. By Newton's third law, we get the opposite of this force in the fluid equations of motion. Of course, if p is constant, the force is zero. Is this also the case for $\hat{p}\hat{\mathbf{n}}|_{\partial\Phi}$? Not in general as we show next. In case p is constant,

$$\begin{aligned}
\overline{p}\nabla\alpha_f &= p\nabla\alpha_f && (3.32)\\
&= p\nabla_{\mathbf{x}}\left(\chi_f * w\right) && (3.33)\\
&= p\nabla_{\mathbf{x}}\int_{\Omega}\chi_f(\mathbf{y},t)w(\mathbf{x}-\mathbf{y})\,d\mathbf{y} && (3.34)\\
&= p\int_{\Omega}\left(\nabla_{\mathbf{y}}\chi_f(\mathbf{y},t)\right)w(\mathbf{x}-\mathbf{y})\,d\mathbf{y} && (3.35)\\
&= -\int_{\partial\Phi(t)} p(\mathbf{y})w(\mathbf{x}-\mathbf{y})\mathbf{n}(\mathbf{y})\,dS && (3.36)\\
&= \hat{p}\hat{\mathbf{n}}|_{\partial\Phi} && (3.37)
\end{aligned}$$

where (3.36) follows form (3.26). We thus conclude that in case of constant pressure, $\overline{p}\nabla\alpha_f$ exactly compensates any nonzero contribution of $\hat{p}\hat{\mathbf{n}}|_{\partial\Phi}$ in (3.31) to give zero, as physically appropriate.

3.2.4. The diffusive term

The last term to tackle is the diffusive term $\mu\Delta\mathbf{v}$. In what follows the constant μ will be left out to decrease the clutter. So we start with the distribution $\chi_f\Delta\mathbf{v}$ and apply the product rule (Theorem 3):

$$\chi_f\Delta\mathbf{v} = \Delta\left(\chi_f\mathbf{v}\right) - 2\nabla\mathbf{v}\cdot\nabla\chi_f - \left(\Delta\chi_f\right)\mathbf{v} \tag{3.38}$$

The first term of (3.38) is the one yielding the Laplacian of $\overline{\mathbf{v}}$ that we were looking for, plus two other terms:

$$\begin{aligned}
\Delta\left(\chi_f\mathbf{v}\right) * w &= \Delta\left(\left(\chi_f\mathbf{v}\right) * w\right) && (3.39)\\
&= \Delta(\alpha_f\overline{\mathbf{v}}) && (3.40)\\
&= \alpha_f\Delta\overline{\mathbf{v}} + 2\nabla\overline{\mathbf{v}}\cdot\nabla\alpha_f + \overline{\mathbf{v}}\Delta\alpha_f && (3.41)
\end{aligned}$$

Now for the rest of (3.38), we need to find out how either

$$\chi_f\Delta\mathbf{v} - \Delta\left(\chi_f\mathbf{v}\right) \qquad \text{or} \qquad -2\nabla\mathbf{v}\cdot\nabla\chi_f - \left(\Delta\chi_f\right)\mathbf{v}$$

act on an arbitrary test function. Deciding for the first option and applying the established rules:

$$\begin{aligned}
\langle \chi_f \Delta \mathbf{v} - \Delta\left(\chi_f \mathbf{v}\right), \varphi \rangle &= \langle \chi_f, \varphi \Delta \mathbf{v} \rangle - \langle \chi_f \mathbf{v}, \Delta \varphi \rangle && (3.42)\\
&= \langle \chi_f, \varphi \Delta \mathbf{v} \rangle - \langle \chi_f, \mathbf{v} \Delta \varphi \rangle \,. && (3.43)\\
&= \langle \chi_f, \varphi \Delta \mathbf{v} - \mathbf{v} \Delta \varphi \rangle && (3.44)\\
&= \int_\Omega \chi_f \left(\varphi \Delta \mathbf{v} - \mathbf{v} \Delta \varphi\right) \, dV && (3.45)\\
&= \int_\Phi \varphi \Delta \mathbf{v} - \mathbf{v} \Delta \varphi \, dV && (3.46)\\
&= \int_{\partial\Phi} (\varphi \nabla \mathbf{v} - \mathbf{v} \otimes \nabla \varphi) \cdot \mathbf{n} \, dS && (3.47)
\end{aligned}$$

where in (3.47) we made use of Green's second identity valid for each component of the vector integral (3.46).
It follows that

$$\begin{aligned}
\left(-2 \nabla \mathbf{v} \cdot \nabla \chi_f - \left(\Delta \chi_f\right) \mathbf{v} \right) * w &= \left(\chi_f \Delta \mathbf{v} - \Delta\left(\chi_f \mathbf{v}\right) \right) * w && (3.48)\\
&= \int_{\partial\Phi} \left(w(\mathbf{x}-\mathbf{y}) \nabla \mathbf{v}(\mathbf{y}) - \mathbf{v} \otimes \nabla_{\mathbf{y}} w(\mathbf{x}-\mathbf{y}) \right) \cdot \mathbf{n}(\mathbf{y}) \, dS && (3.49)
\end{aligned}$$

The first term of (3.49) represents the weighted average of the stress at the interface. Analogously to the pressure, we use the notation

$$\widehat{\nabla \mathbf{v} \cdot \hat{\mathbf{n}}}|_{\partial\Phi} := \int_{\partial\Phi} \left(w(\mathbf{x}-\mathbf{y}) \nabla \mathbf{v}(\mathbf{y}) \right) \cdot \mathbf{n}(\mathbf{y}) \, dS$$

and also introduce

$$\overrightarrow{\mathbf{v} \cdot \hat{\mathbf{n}}}|_{\partial\Phi} := \int_{\partial\Phi} \left(\mathbf{v} \otimes \nabla_{\mathbf{y}} w(\mathbf{x}-\mathbf{y}) \right) \cdot \mathbf{n}(\mathbf{y}) \, dS$$

where $\hat{\mathbf{n}} = -\mathbf{n}$ is the vector pointing into the fluid phase.
We have no obvious interpretation for the second term, postulating that it again combines with terms in (3.41) to give zero in case $\nabla \mathbf{v} = 0$ (zero shear stress), as it was the case in (3.31). Collecting the terms, the phasic averaging of the diffusive term reads:

$$\left(\chi_f \mu \Delta \mathbf{v}\right) * w = \mu \left[\alpha_f \Delta \overline{\mathbf{v}} + 2 \nabla \overline{\mathbf{v}} \cdot \nabla \alpha_f + \overline{\mathbf{v}} \Delta \alpha_f - \widehat{\nabla \mathbf{v} \cdot \hat{\mathbf{n}}}|_{\partial\Phi} + \overrightarrow{\mathbf{v} \cdot \hat{\mathbf{n}}}|_{\partial\Phi} \right] \tag{3.50}$$

3.3. Summary and force models

Collecting all the terms, we have arrived at the following equation:

$$\rho \frac{\partial}{\partial t}\left(\alpha_f \overline{\mathbf{v}}\right) + \rho \operatorname{div}\left(\alpha_f \overline{\mathbf{v}} \otimes \overline{\mathbf{v}}\right) - \rho \operatorname{div}(\alpha_f \mathcal{R}_c) = -\alpha_f \nabla \overline{p} + \alpha_f \Delta \overline{\mathbf{v}} + \alpha_f \rho \mathbf{g} + \mathcal{R}_{RHS} \tag{3.51}$$

where

$$\mathcal{R}_{RHS} = -\overline{p}\nabla\alpha_f + \hat{p}\hat{\mathbf{n}}|_{\partial\Phi} + 2\mu\left(\nabla\overline{\mathbf{v}}\cdot\nabla\alpha_f\right) + \mu\overline{\mathbf{v}}\Delta\alpha_f + \mu\widehat{\nabla\mathbf{v}\cdot\hat{\mathbf{n}}}|_{\partial\Phi} - \mu\overrightarrow{\mathbf{v}\cdot\hat{\mathbf{n}}}|_{\partial\Phi} \quad (3.52)$$

The current practice in engineering is to replace $\mathcal{R}_{RHS}$ by force models, whereas the term $-\rho\,\mathrm{div}(\alpha_f\mathcal{R}_c)$ is not mentioned at all. [9] [10]. The literature distinguishes about 7 distinct means of momentum exchange between a particle and the fluid in which it is suspended. For example, [9] writes the total force on the particle $\mathbf{F}_{pf}$ as:

$$\mathbf{F}_{pf} = \mathbf{F}_D + \mathbf{F}_{\nabla p} + \mathbf{F}_{\mathrm{div}\,\tau} + \mathbf{F}_{vm} + \mathbf{F}_{Basset} + \mathbf{F}_{Saffman} + \mathbf{F}_{Magnus} \quad (3.53)$$

where $\mathbf{F}_D$ is the drag force, $\mathbf{F}_{\nabla p}$ is the pressure gradient force, $\mathbf{F}_{\mathrm{div}\,\tau}$ is the fluid shear stress force, $\mathbf{F}_{vm}$ is the virtual mass force and the other three forces are named by their discoverers. Establishing links between the terms in (3.52) and (3.53) is an open question. Depending on the flow conditions, a subset of these forces can typically be neglected. When modeling gas-particle flows which are characterized by $\rho_p \gg \rho_f$ at moderate velocities and accelerations, it is customary to consider just the $\mathbf{F}_D$ and $\mathbf{F}_{\nabla p}$ [11] or even just $\mathbf{F}_D$ [12] when buoyancy can be neglected. Whereas the pressure $\mathbf{F}_{\nabla p}$ is relatively easy to evaluate, a *force model* needs to be supplied for $\mathbf{F}_D$. The universally accepted drag equation for a single particle [13] reads:

$$\mathbf{F}_D = \frac{1}{2}C_D\rho A\|\mathbf{v}_{f\infty} - \mathbf{v}_p\|\mathbf{v}_{f\infty} - \mathbf{v}_p \quad (3.54)$$

where A is the area of the particle projected in the direction of the flow and C_D is the dimensionless drag coefficient which is generally a complicated function of $\mathbf{v}_{rel}, \mathrm{Re}_p$, α_f and the particle sphericity ς defined as

$$\varsigma = \frac{A_{sphere}}{A_{particle}}$$

where A_{sphere} is the area of a sphere which has the same volume as the particle and $A_{particle}$ the surface area of the particle. To illustrate, the drag coefficient due to Huilin and Gidaspow [14] [15] reads:

$$C_D = \psi C_{D_1} + (1-\psi)C_{D_2} \quad (3.55)$$

where

$$C_{D_1} = \frac{200\alpha_s}{\alpha_f\phi^2\,\mathrm{Re}_p} + \frac{7}{3\phi} \quad (3.56)$$

$$C_{D_2} = \alpha_f^{-1.65}\max\left\{\frac{24}{\alpha_f\,\mathrm{Re}_p}\left[1 + 0.15\left(\alpha_f\,\mathrm{Re}_p\right)^{0.687}\right], 0.44\right\} \quad (3.57)$$

and ψ is given by:

$$\psi = \frac{1}{\pi}\arctan\left[150\cdot 1.75\left(0.8-\alpha_f\right)\right] + 0.5.$$

4. Calculating the volume fraction in the context of the finite volume method

We have thus arrived at the VANS system for an incompressible fluid mixed with a particle phase:

$$\frac{\partial \alpha_f}{\partial t} + \operatorname{div}(\alpha_f \overline{\mathbf{v}}) = 0 \tag{4.1}$$

$$\frac{\partial}{\partial t}\left(\rho \alpha_f \overline{\mathbf{v}}\right) + \operatorname{div}\left(\rho \alpha_f \overline{\mathbf{v}} \otimes \overline{\mathbf{v}}\right) = -\alpha_f \nabla \overline{p} + \alpha_f \mu \Delta \overline{\mathbf{v}} + \rho \alpha_f \mathbf{g} - \mathbf{F}_{fs}. \tag{4.2}$$

Comparing it to the incompressible Navier-Stokes system:

$$\operatorname{div} \mathbf{v} = 0 \tag{4.3}$$

$$\frac{\partial (\rho \mathbf{v})}{\partial t} + \operatorname{div}(\rho \mathbf{v} \otimes \mathbf{v}) = -\nabla p + \mu \Delta \mathbf{v} + \rho \mathbf{g}, \tag{4.4}$$

we see that the main difference is the occurrence of α_f in the equations. Indeed, setting $\alpha_f = 1$ and $\mathbf{F}_{fs} = 0$ we recover (4.3) and (4.4).
Based on the positions of the particles at a given time-step as provided by the DEM solver, it is possible to compute the volume fraction of the solid phase α_s. The volume fraction of the fluid phase is then given by $\alpha_f = 1 - \alpha_s$.
Once α_f is known, the VANS system consists of 4 equations (continuity and the three components of the averaged velocity) with 4 unknowns (the three averaged velocity components and pressure). Thus we turn to the topic of calculating α_s and do this in the context of the finite volume method.

4.1. Summary of the finite volume method

The most widely used discretization method in CFD is the Finite volume method (FVM), developed in the period from mid 1960s to mid 1970s by Spalding and Patankar. A general contemporary reference for FVM is [16], which also serves as a source for this section. We briefly recall the main steps of the FVM:

1. Divide the domain into *finite volumes*, also called *cells*, such that each cell C with volume V_C has a set of neighboring cells $\mathcal{N}_C$ and a set of faces $\mathcal{F}_C$ such that it shares exactly one face F of surface area S_F with each neighbor.

2. Write down a balance equation in integral form for each conserved scalar quantity and for each cell, which serves as a control volume (see appendix B). Consider

equation (4.2), which expresses the conservation of momentum in the presence of the transient, convective, diffusive and source terms. The balance over a cell takes the form:

$$\begin{aligned}\int_t^{t+\Delta t}\int_{V_c}\frac{\partial(\rho\alpha_f\phi)}{\partial t}dV\,dt + \int_t^{t+\Delta t}\left[\sum_{F\in\mathcal{F}_C}\left(\int_F(\rho\alpha_f\overline{\mathbf{v}}\phi)\cdot\mathbf{n}dS\right)\right]dt \\ -\int_t^{t+\Delta t}\left[\sum_{F\in\mathcal{F}_C}\left(\int_F(\alpha_f\mu\nabla\phi)\cdot\mathbf{n}dS\right)\right]dt \\ =\int_t^{t+\Delta t}\left[\int_{V_c}Q^\phi dV\right]dt\end{aligned} \tag{4.5}$$

where ϕ is one of the three velocity components and the source term Q^ϕ contains all the terms which do not involve the velocity. The equations for individual cells are coupled by the fluxes across the shared faces, which must be equal.

3. Choose a numerical method by which to evaluate the volume and surface integrals; this yields a system of equations at a finite number of points (the integration nodes). The usual approach is to choose one integration node: the centroid of the cell for volume integrals and of the face for surface integrals, respectively. Let $\mathbf{x}_C$ be the centroid of a cell and $\mathbf{x}_F$ the centroid of a face, defined as

$$\mathbf{x}_C = \frac{\int_C \mathbf{x}\,dV}{V_C} \qquad \mathbf{x}_F = \frac{\int_F \mathbf{x}\,dS}{S_F}. \tag{4.6}$$

For an arbitrary function ψ we have

$$\int_{V_C}\psi\,dV = \int_{V_C}\left[\psi(\mathbf{x}_C)+(\mathbf{x}-\mathbf{x}_C)\cdot\nabla\psi|_{\mathbf{x}_C}+O\left(|\mathbf{x}-\mathbf{x}_C|^2\right)\right]dV \tag{4.7}$$

$$=\psi(\mathbf{x}_C)\int_{V_C}dV+\int_{V_C}(\mathbf{x}-\mathbf{x}_C)\cdot\nabla\psi|_{\mathbf{x}_C}\,dV+\int_{V_C}O\left(|\mathbf{x}-\mathbf{x}_C|^2\right)dV \tag{4.8}$$

$$=\psi(\mathbf{x}_C)V_C+O\left(|\mathbf{x}-\mathbf{x}_C|^2\right), \tag{4.9}$$

yielding a method second order accurate in the cell radius. An analogous expression also holds for the surface integral over a cell face. Using this method in (4.5), we get

$$\begin{aligned}\int_t^{t+\Delta t}V_C\frac{\partial(\rho\alpha_f\phi)}{\partial t}\Big|_{\mathbf{x}_C}dt+\int_t^{t+\Delta t}\left[\sum_{F\in\mathcal{F}_C}\left((\rho\alpha_f\overline{\mathbf{v}}\phi)\big|_{\mathbf{x}_F}\cdot\mathbf{n}S_F\right)\right]dt \\ -\int_t^{t+\Delta t}\left[\sum_{F\in\mathcal{F}_C}\left((\alpha_f\mu\nabla\phi)\big|_{\mathbf{x}_F}\cdot\mathbf{n}S_F\right)\right]dt \\ =\int_t^{t+\Delta t}\left[Q^\phi\big|_{\mathbf{x}_C}V_C\right]dt\end{aligned} \tag{4.10}$$

4. Express the function values at the cell faces in terms of the ones at the cell centroids by means of interpolation or extrapolation and also choose a method of evaluating the derivatives.

5. Choose a time advancement algorithm.

It is at the integration nodes where the values of α_f are needed, and based on these $\nabla\alpha_f$ and $\frac{\partial\alpha_f}{\partial t}$ can also be evaluated.

4.2. Methods for calculating the volume fraction

A number of ways of calculating α_s have been proposed and the topic is still the subject of ongoing investigations [10]. The statement of the problem is simple: for each integration node $\mathbf{x}$, find α_s given the particles $P_i, i = 1 \dots N$ with centroids $\mathbf{c}_i$ and volumes V_i at a given time-step. The shapes and orientations of the particles in space are usually disregarded when calculating α_s, which can be attributed to the fact that large-scale DEM calculations often use spherical particles as an approximation [9]. Calculating α_s accurately is of crucial importance not only for the VANS equations but also for other models which build on top of unresolved CFD-DEM, and deal with physical phenomena such as heat transfer, phase-change, radiation et cetera.

4.2.1. The particle counting method

This is the standard method used both in the literature and in the applications [10] [17]. For each cell C_j with cell centroid $\mathbf{x}_{C_j}$ and volume V_{C_j}, evaluate

$$\alpha_s(\mathbf{x}_{C_j}) = \frac{\sum\limits_{\mathbf{c}_i \in C_j} V_i}{V_{C_j}} \tag{4.11}$$

The advantages of this method are that it is easy to implement and is conservative in the sense that:

$$\sum_{j=1}^{M} \alpha_s(\mathbf{x}_{C_j}) V_{C_j} = \sum_{i=1}^{N} V_i \tag{4.12}$$

However it also suffers major drawbacks. Firstly, there are many possibilities for the unphysical situation where $\alpha_{PCM} > 1$, especially if the domain contains cells with a volume smaller than the volume of the largest particle. Meshes are often required to have such cells in some parts of the domain in order to capture flow near walls or complex features of the domain. Moreover, a stricter upper bound

$$\alpha_s(\mathbf{x}_{C_j}) < \alpha_{max} \tag{4.13}$$

is usually required, where in the case of identical particles, α_{max} is the *packing constant* of the particle and in the case of non-identical particles, α_{max} is the packing constant

of the particle distribution. The packing constant of most geometric shapes is in fact unknown [18], but it can be estimated. For cells which do not satisfy (4.13), the following approach is usually taken [10]:

Diffusion smoothing

For all j where $\alpha_s(\mathbf{x}_{C_j}) > \alpha_{max}$, solve

$$\frac{\partial \alpha(\mathbf{x}_{C_j})}{\partial t} = D\Delta\alpha(\mathbf{x}_{C_j}) \tag{4.14}$$

until $\alpha_j \leq \alpha_{max}$ for all j. On a homogeneous mesh, 4.14 may be discretized as:

$$\frac{\alpha^{k+1} - \alpha^k}{\Delta t} = \frac{D}{(\Delta x)^2} \sum_{n \in \mathcal{N}} \left(\alpha_n - \alpha(\mathbf{x}_{C_j})\right) \tag{4.15}$$

Secondly, recalling definition (7), we recognize that (4.11) corresponds to using the indicator function of the cell C_j as the weight function, up to the error arising from the particles at the cell border, which generally cancels out. This violates the differentiability requirements on w and also in general corresponds to an inhomogeneous averaging, since the vast majority of meshes for practical problems are not homogeneous. Thirdly, this approach only finds α at the cell centroids and interpolation is needed to then find α at all the other nodes. Lastly, in the case when (4.13) is always satisfied and no smoothing is triggered, an error is introduced as we show next.

Perturbed mesh test

We would like to test the how the aforementioned properties of this method influence the solution. To this end we solve the VANS equations in 2D on the rectangular domain $[0, 1] \times [0, 1]$ in the presence of two randomly generated particle clouds drawn from uniform distributions, see figure 4.1 (a). The idea of this test is to solve the problem on two slightly different meshes: one is a homogeneous cartesian mesh of 10×10 cells and the other is a *perturbed* version, where we introduce a perturbation in the x-direction, uniformly distributed in $[-0.04, 0.04]$. This thus allows for a difference in the edge length between the cells of the two meshes of up to 8%, see figure 4.1 (b). As expected, when using the particle counting method, the two meshes give slightly different values of α_s, displayed in figure 4.2.

It is then interesting to see how this slightly different volume fraction field affects the fluid flow solution. To focus on the flow problem, we will solve the equations in the limit of $m_p \to \infty$. That is, there will be a force acting on the particles by the fluid but on the time scale of our problem the particles will not be accelerated at all. The initial velocity of all particles is set to zero. We use the drag law introduced in [14] as implemented in the Ansys-Rocky DEM solver [15]. The following boundary and initial conditions,

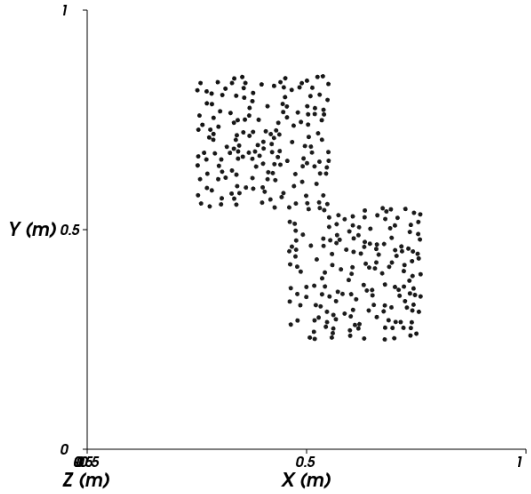

(a) Two particle swarms

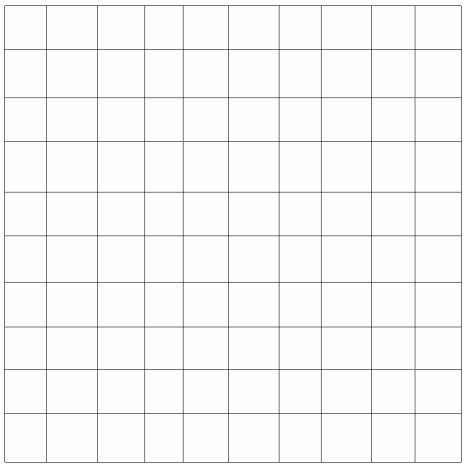

(b) A mesh slightly parturbed in the x-direction

Figure 4.1.: The setup of wiggled mesh test

denoting $\mathbf{x} = [x_1, x_2]$, were used:

$$\begin{aligned} \overline{\mathbf{v}}(\mathbf{x}) &= [-2, 0] \qquad \{\mathbf{x} \,|\, x_1 = 1\} \\ \overline{\mathbf{v}}(\mathbf{x}) &= [0, 0] \qquad \{\mathbf{x} \,|\, x_2 = 0\} \\ \overline{\mathbf{v}}(\mathbf{x}) &= [0, 0] \qquad \{\mathbf{x} \,|\, x_2 = 1\} \\ p(\mathbf{x}) &= 0 \qquad \{\mathbf{x} \,|\, x_1 = 0\} \\ \overline{\mathbf{v}}(\mathbf{x}, t = 0) &= [0, 0] \\ p(\mathbf{x}, t = 0) &= 0 \end{aligned}$$

The standard pressure-based solver implemented in Ansys-Fluent [21] was used with the following choices for spatial discretization:

	Method	Formula
Gradient	Least squares cell based	see equation (4.20)
Pressure interp.	Second order finite diff.	see equation (4.16)
Momentum interp.	Second order upwind	$v_i(\mathbf{x}_F) = v_i(\mathbf{x}_U) + \nabla v_i(\mathbf{x}_U) \cdot (\mathbf{x}_F - \mathbf{x}_U)$

Where $\mathbf{x}_U$ denotes the centroid of the cell *upwind* of the face F.

$$p(\mathbf{x}_{F_{01}}) = \frac{p(\mathbf{x}_{C_0}) + p(\mathbf{x}_{C_1})}{2} + \frac{\nabla p(\mathbf{x}_{C_0}) \cdot (\mathbf{x}_{F_{01}} - \mathbf{x}_{C_0}) + \nabla p(\mathbf{x}_{C_1}) \cdot (\mathbf{x}_{F_{01}} - \mathbf{x}_{C_1})}{2} \tag{4.16}$$

Figure 4.2.: Comparison of the volume fraction values at the cell centers obtained by the particle counting method. Left: wiggled grid, right: regular cartesian grid.

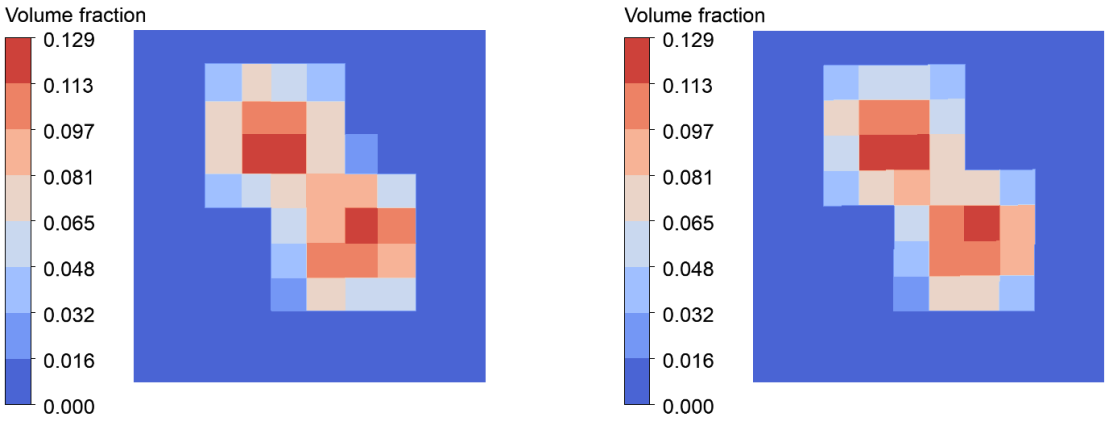

Least squares gradient

Assuming that the solution between two cell centroids can be well approximated by a linear function, we can express the gradient as:

$$(\mathbf{x}_{C_i} - \mathbf{x}_{C_0}) \cdot \nabla\phi(\mathbf{x}_{C_0}) = \phi(\mathbf{x}_{C_i}) - \phi(\mathbf{x}_{C_0}) \qquad i = 1, \ldots, m \tag{4.17}$$

for a cell with m neighbors. Cells in $\mathbb{R}^n$ always have at least $n+1$ neighbors, so (4.17) is an over-determined linear system, expressed in matrix form as

$$\mathbf{A}\nabla\boldsymbol{\phi} = \delta\boldsymbol{\phi} \tag{4.18}$$

which may at best be solved in the sense of finding[1]

$$\nabla\boldsymbol{\phi}_{LS} := \min_{\nabla\boldsymbol{\phi}} \|\mathbf{A}\nabla\boldsymbol{\phi} - \delta\boldsymbol{\phi}\|_2^2 . \tag{4.20}$$

For the time advancement, the fractional step method [20] was used, as implemented in Ansys-Fluent [21] with the constant step-size of $0.001s$. After 2000 time-steps, the flow field reaches a pseudosteady-state, shown in figure 4.3. We see that although being qualitatively similar, the results of the two cases are significantly different in the bottom part of the domain, despite the fact that they represent the same physical situation.

[1] Since mesh cells with a high skewness often occur in practice (resulting in the rows of $\mathbf{A}$ being close to linearly dependent) and algorithms for solving the normal equations

$$\mathbf{A}^T\mathbf{A}\nabla\boldsymbol{\phi} = \mathbf{A}^T\delta\boldsymbol{\phi} \tag{4.19}$$

are not stable in the presence of rounding errors [19], the system is usually solved by obtaining the reduced QR factorization of $\mathbf{A}$.

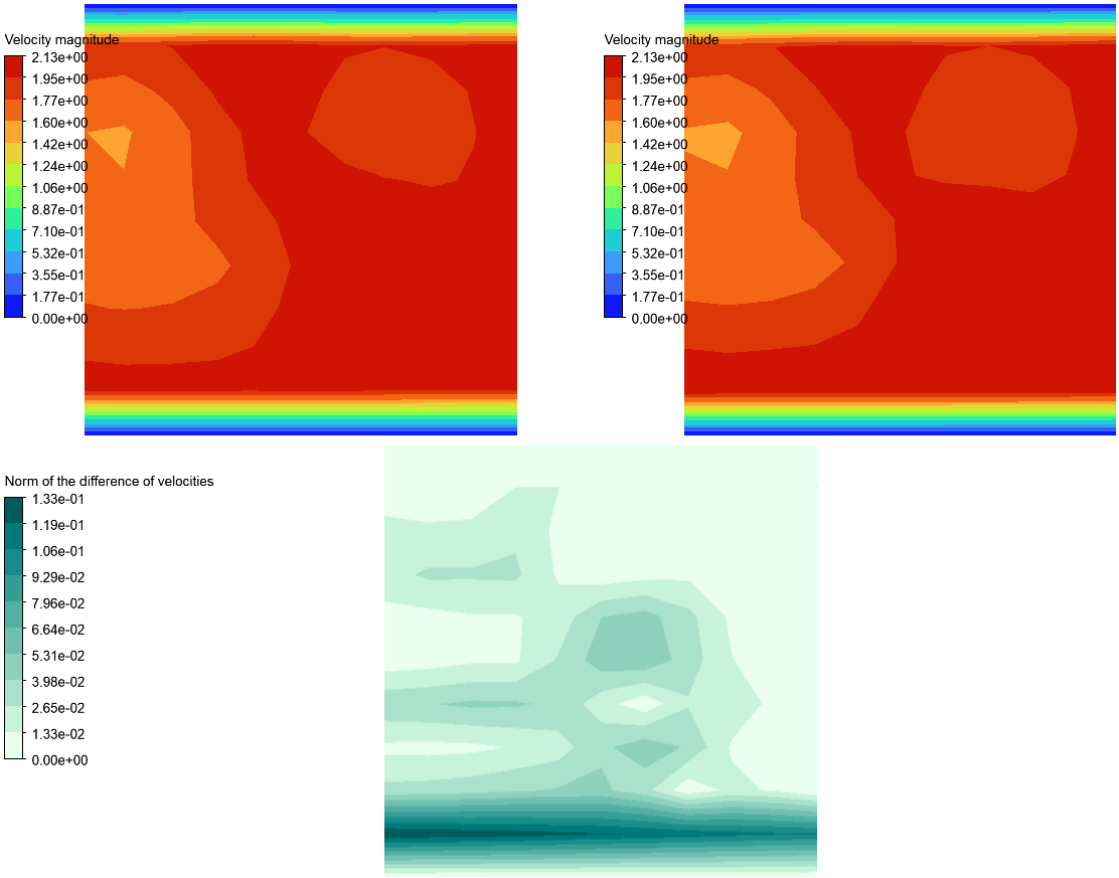

Figure 4.3.: Comparison of the velocity in the wiggled mesh test. Top left: $\|\mathbf{v}_{left}\|_2$ on a wiggled grid, top right: $\|\mathbf{v}_{right}\|_2$ on a regular cartesian grid, bottom: $\|\mathbf{v}_{left} - \mathbf{v}_{right}\|_2$

4.2.2. Divided particle volume methods

This family of methods divide the volume of each particle into the cells in its vicinity, in such a way that (4.12) is satisfied [22]. The most common versions aim to divide the volume exactly [23]. Others associate a probability distribution with a given radius which is usually greater than the particle radius and distribute the particle volume to a the cells within the radius based on the amount of overlap with a given cell. For example, [17] uses a Gaussian of the form:

$$g\left(\mathbf{x} - \mathbf{c}_i, R_i\right) = \frac{2}{3\pi R_i^3} \exp\left(-\left\|\mathbf{x} - \mathbf{c}_i\right\|_2^2 / R_i^2\right). \tag{4.21}$$

4.2.3. The numerical convolution method

We are not aware of methods which would actually attempt to evaluate the integral in definition (7) numerically. Choose a weight function w of radius r and denote by $B_r(\mathbf{x}_j)$ the n-sphere of radius r around the node $\mathbf{x}_j$. Let I_j be the set of indices of the particles which intersect $B_r(\mathbf{x}_j)$ and $\tilde{I}_j$ the set of indices of the particles whose centroids lie in $B_r(\mathbf{x}_j)$. For each $\mathbf{x}_j$, evaluate

$$\alpha_s(\mathbf{x}_j) = \chi_s * w = \int_\Omega \chi_s(\mathbf{y}) w(\mathbf{x}_j - \mathbf{y})\, d\mathbf{y} \tag{4.22}$$

$$= \sum_{i \in I_j} \int_{P_i} w(\mathbf{x}_j - \mathbf{y})\, d\mathbf{y} \tag{4.23}$$

$$\approx \sum_{i \in \tilde{I}_j} w(\mathbf{x}_j - \mathbf{c}_i)\, V_{P_i} \tag{4.24}$$

Provided that the particles are approximately spherical, (4.24) is an excellent approximation to the midpoint rule. This method offers several advantages:

- Direct evaluation at points of interest, no need for interpolation to the cell faces
- Values obtained change continuously as a function of the node position
- Suitability for mesh cells of arbitrary shape and size
- No need for modifications when used with higher order FVM, which uses more integration nodes in step 3. of the FVM procedure

The drawback is that the method is not strictly conservative in the sense of (4.12). It is a question whether this requirement is too restrictive. We suggest that a method need only be conservative in the appropriate limit. Denoting by V_{max} the maximum cell volume on a given mesh, the requirement would be

$$\lim_{V_{max} \to 0} \sum_j \alpha_s(\mathbf{x}_{C_j}) V_{C_j} = \sum_{i=1}^{N} V_i. \tag{4.25}$$

We test the method in $\mathbb{R}^2$, using the function from definition (5) with $\varepsilon = 1$ as w, see figure 4.4. First we use a uniform particle size and an average solid fraction of about 0.2, see figure 4.5. The test of the validity of 4.25 is shown figure 4.6. We see that the sum does converge, albeit to a value slightly lower than the exact average solid volume fraction. The norm of the relative error also increases from a certain point as $d \to 0$ but nevertheless remains within 1% across an order of magnitude, see figure 4.7. This is likely due to summing over $\tilde{I}_j$ in 4.24 and disregarding the particles which have an overlap smaller than their radius with the support of w.

Figure 4.4.: Graph of the function from definition (5) in 2D with $\varepsilon = 1$

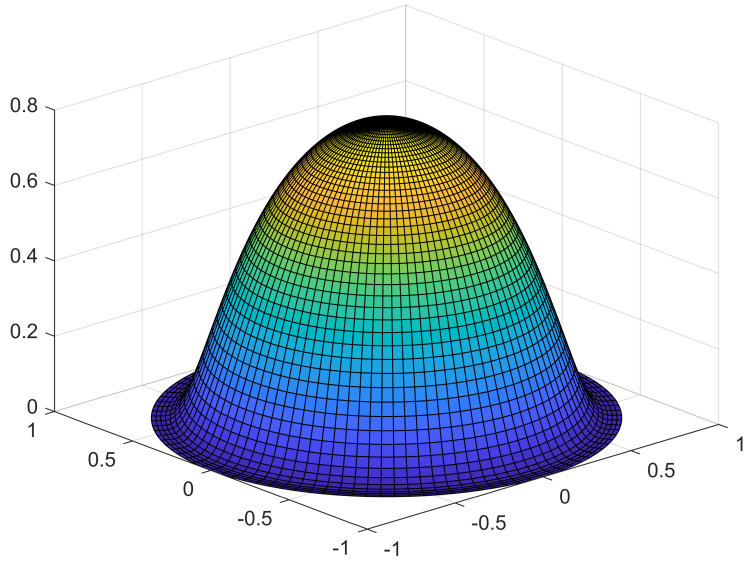

Figure 4.5.: Random particle distribution on a mesh with an inflation layer

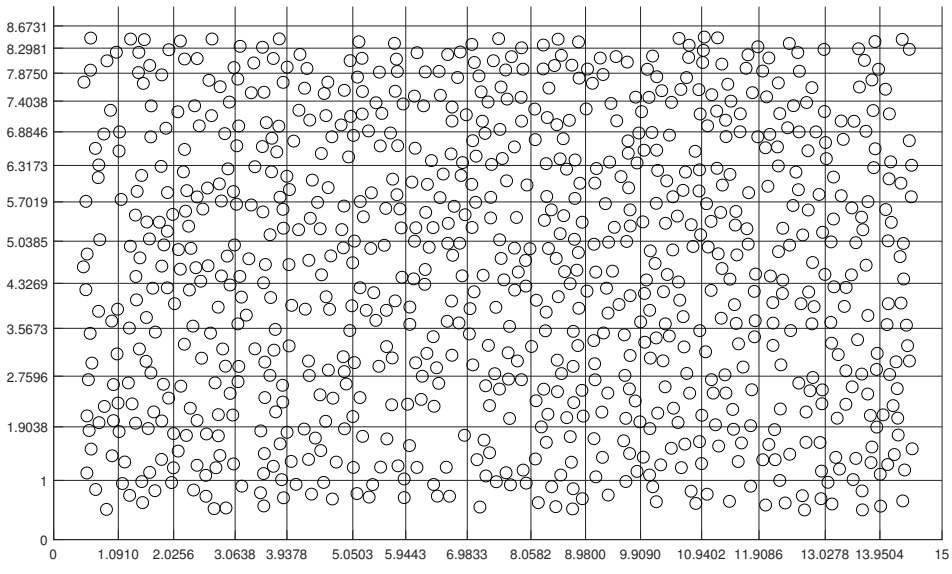

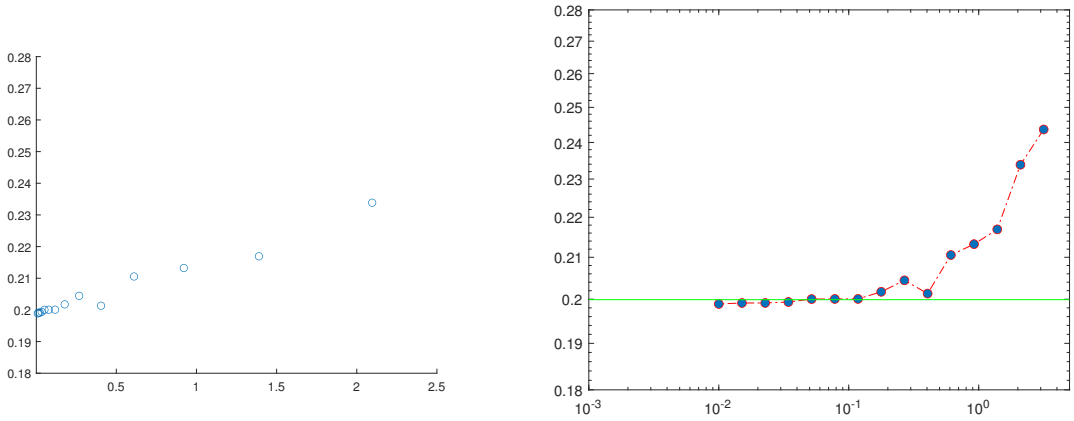

(a) On a linear scale (b) On a logarithmic scale

Figure 4.6.: Convergence of the average volume fraction as a function of cell diameter. The green horizontal line represents the exact average over the whole domain.

Figure 4.7.: Norm of the relative error as $d \to 0$.

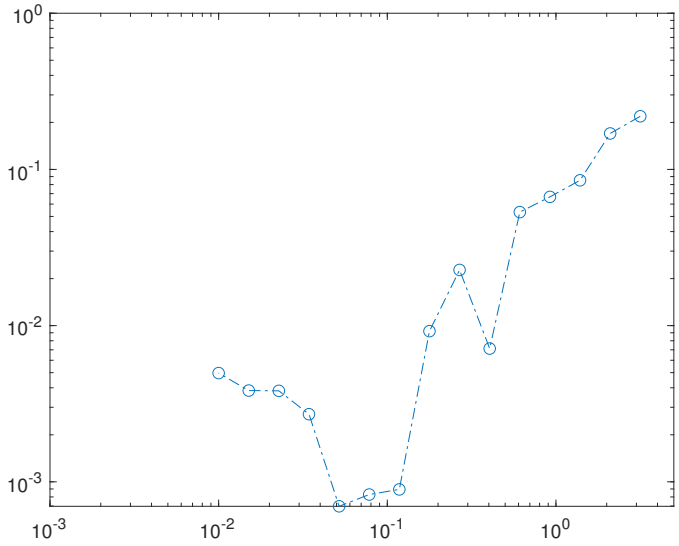

The contour plots of α_s for a few selected values of d are shown in figure 4.8.

Figure 4.8.: Contour plots of α_s for the particle cloud in figure 4.5 and various values of the cell diameter

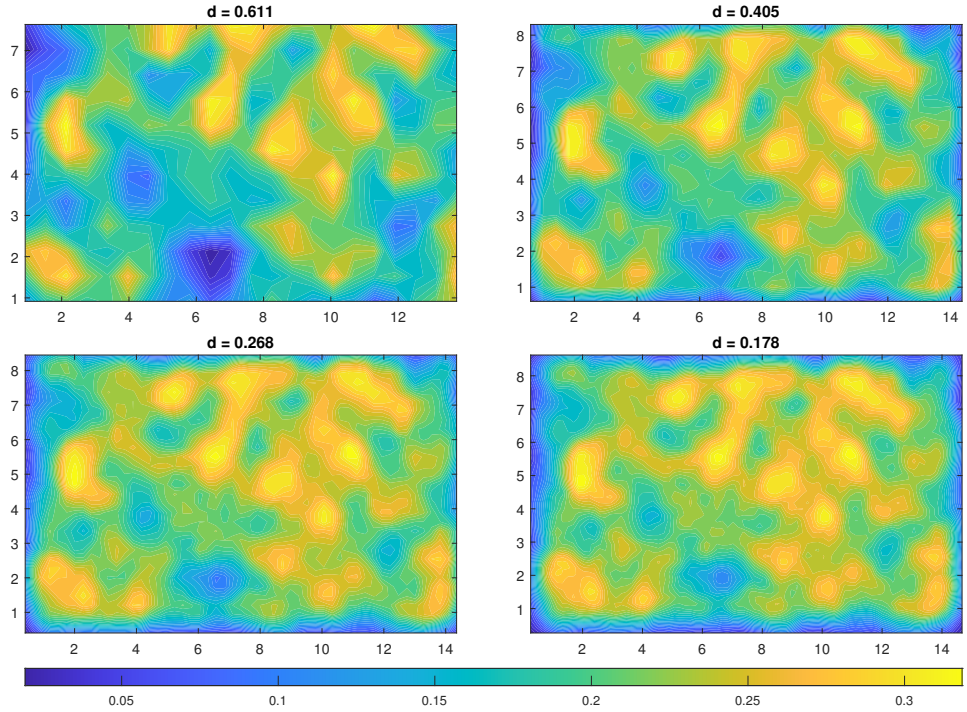

Figure 4.9.: Filled contour plot of α_s for the situation in figure 4.5 with the nodes marked by '+'.

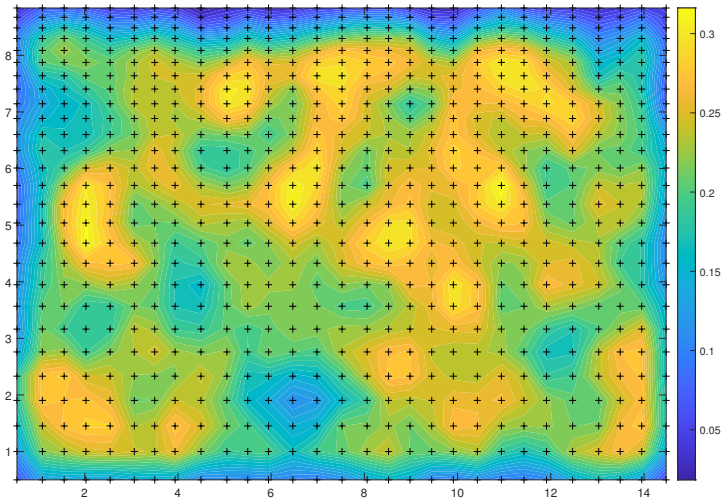

The mesh was purposefully chosen with a successive refinement near the walls of the domain, so called *mesh inflation*. This is necessary to capture the *boundary layer* near the wall accurately. Estimating the boundary layer thickness and shape is a major topic of fluid mechanics [24]. What matters for unresolved CFD-DEM is that the situations where the particle diameter is smaller than the boundary layer thickness but larger than the cell volumes in the boundary layer do occur in practice, which leads to violation of (4.13) when the particle counting method is used and the need for additional smoothing. The numerical convolution method performed well in this case, capturing a accurately a distribution of particle sizes shown in figure 4.10 and conserving the total solid volume fraction up to a small error, see figures 4.11 through 4.14.

Figure 4.10.: Random particle distribution on a mesh with an inflation layer

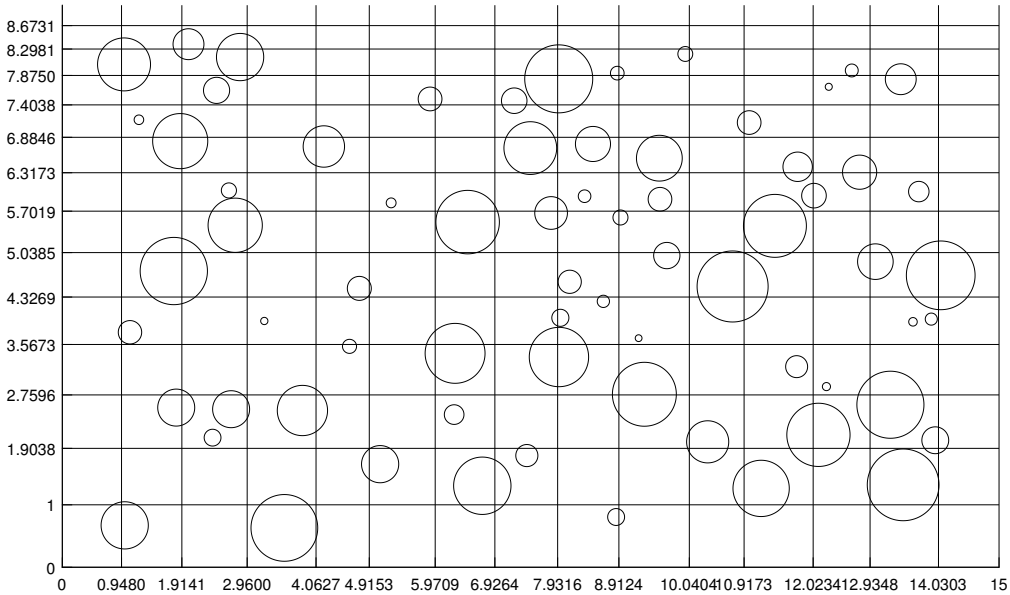

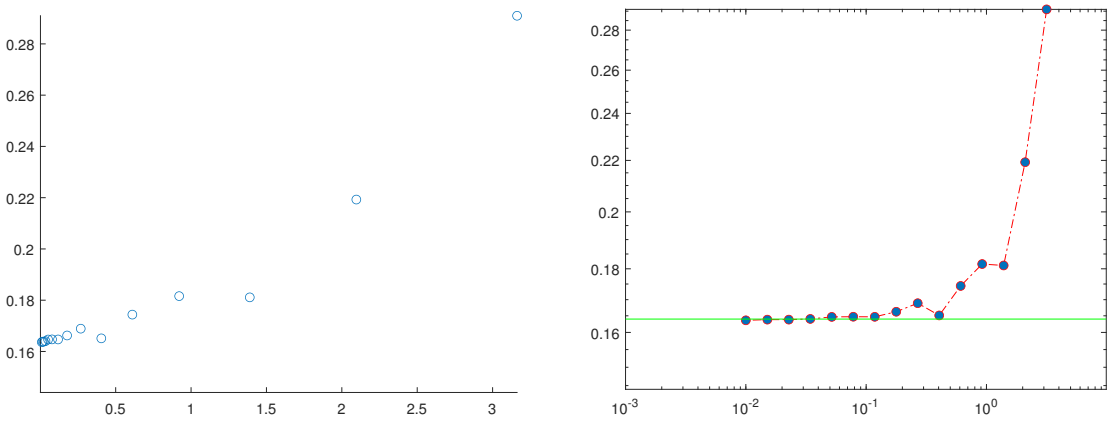

(a) On a linear scale (b) On a logarithmic scale

Figure 4.11.: Convergence of the average volume fraction as a function of cell diameter. The green horizontal line represents the exact average over the whole domain.

Figure 4.12.: Norm of the relative error as $d \to 0$.

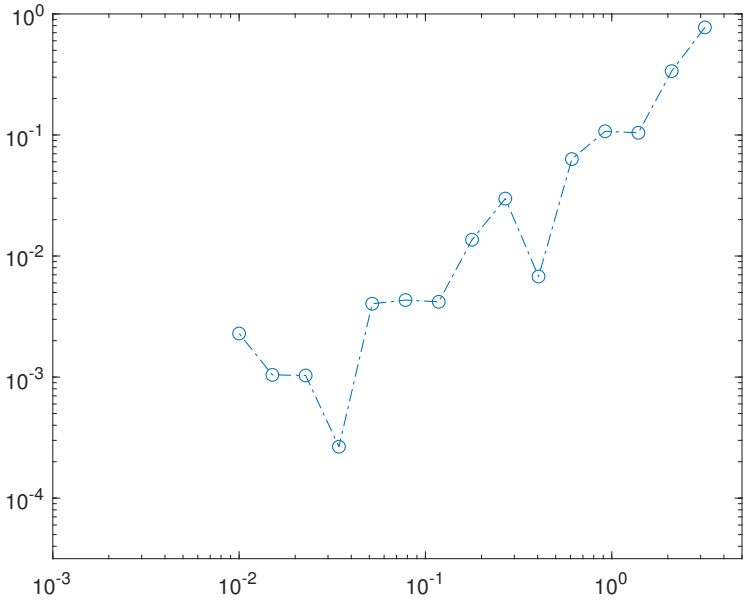

Figure 4.13.: Contour plots of α_s for the particle cloud in figure 4.10 and various values of the cell diameter

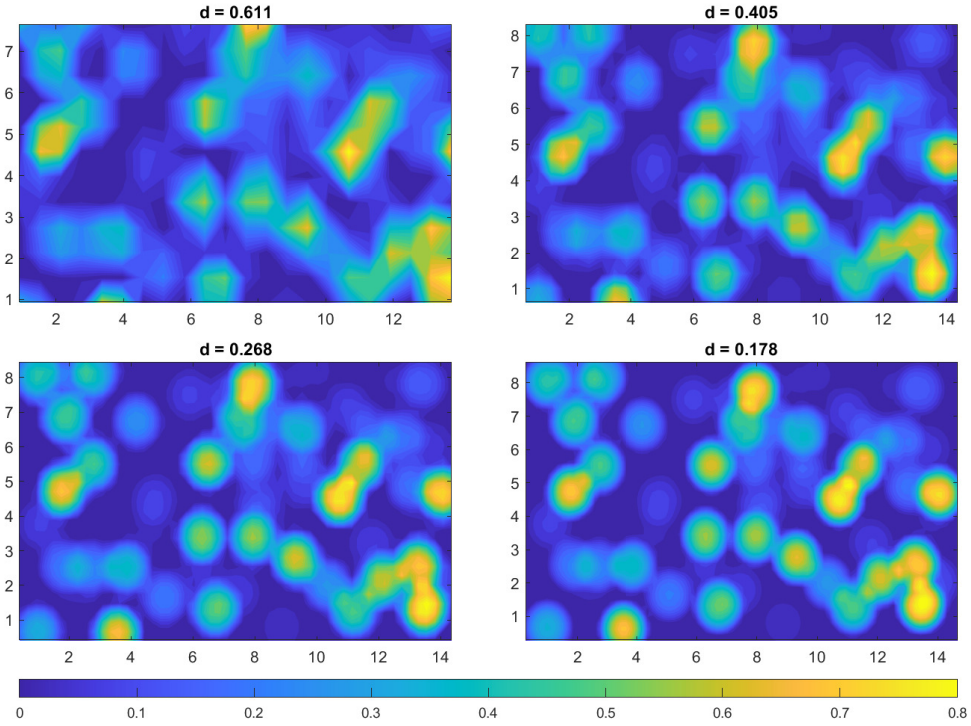

Figure 4.14.: Filled contour plot of α_s for the situation in figure 4.10 with the nodes marked by '+'.

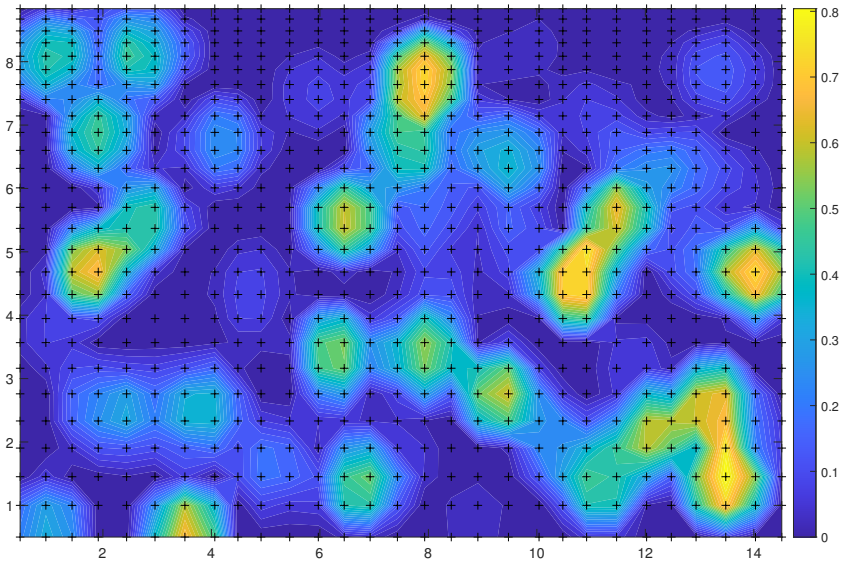

5. Conclusions

In summary, we have explored the method of unresolved CFD-DEM by first putting it into context and comparing it to similar methods used to solve the problems of multiphase flow. Next, after presenting the appropriate mathematical tools, they were used to derive the incompressible volume-averaged Navier-Stokes equations for a single fluid phase mixed with a solid phase. Many extra terms have appeared in the process. We postulate that the fact that they are disregarded in practice partly explains the complicated expressions for particle-fluid interaction forces, which then provide the necessary correction mechanism.
Next we looked at the most common way to solve the equations in practice, the finite volume method, and focused on the topic of computing the volume fraction in this context. After looking at the standard way of doing so, we tested it numerically by a perturbed mesh test and measured the effect on the flow field. Then we proposed a way to compute the volume fraction by directly evaluating its definition numerically. We saw that this method is conservative only in the limit of zero cell size but conserves the volume fraction up to a small error on typical meshes.
Some directions for future work might be, firstly, establishing links between the extra terms arising due to averaging and the single-particle force models. And secondly, implementing the new volume fraction calculation method into a solver based on the finite-volume discretization.

A. Notation and useful identities

We will prefer to write equations in vector form rather than in component form, except when proving identities (which then hold in an arbitrary basis). For our purposes it is not necessary to distinguish between covariant and contravariant tensors so all our tensors will have lower indices. It is assumed that we have picked an orthonormal basis $\mathbf{e}_i \cdot \mathbf{e}_j = \delta_{ij}$ where δ_{ij} is the Kronecker delta. Lowercase boldface letters are reserved for vectors (first-order tensors):

$$\mathbf{a} = \sum_i a_i \mathbf{e}_i \qquad \text{so that} \qquad \mathbf{a} \cdot \mathbf{b} = \sum_i a_i b_i \mathbf{e}_i \cdot \mathbf{e}_i = \sum_i a_i b_i,$$

whereas uppercase boldface letters for second-order tensors, which are the only kinds of tensors of order > 1 we will need. They can be represented in a basis of *unit dyads* $\mathbf{e}_i \otimes \mathbf{e}_j$.

$$\mathbf{A} = \sum_i \sum_j A_{ij} \mathbf{e}_i \otimes \mathbf{e}_j.$$

We have

$$\mathbf{e}_i \otimes \mathbf{e}_j \cdot \mathbf{e}_k = \delta_{jk} \mathbf{e}_i$$
$$\mathbf{e}_k \cdot \mathbf{e}_i \otimes \mathbf{e}_j = \delta_{ki} \mathbf{e}_j$$

so that in general $\mathbf{A} \cdot \mathbf{b} \neq \mathbf{b} \cdot \mathbf{A}$:

$$\mathbf{A} \cdot \mathbf{b} = \sum_i \sum_j \sum_k A_{ij} b_k \left(\mathbf{e}_i \otimes \mathbf{e}_j \cdot \mathbf{e}_k \right) = \sum_i \sum_j \sum_k A_{ij} b_k \delta_{jk} \mathbf{e}_i = \sum_i \sum_j b_i A_{ji} \mathbf{e}_j$$
$$\mathbf{b} \cdot \mathbf{A} = \sum_i \sum_j \sum_k b_k A_{ij} \left(\mathbf{e}_k \cdot \mathbf{e}_i \otimes \mathbf{e}_j \right) = \sum_i \sum_j \sum_k b_k A_{ij} \delta_{ik} \mathbf{e}_j = \sum_i \sum_j b_i A_{ij} \mathbf{e}_j$$

unless $\mathbf{A}$ is symmetric, as is the case when $\mathbf{A} = \mathbf{a} \otimes \mathbf{a} = \sum_i \sum_j a_i a_j \mathbf{e}_i \otimes \mathbf{e}_j$.
Associativity does hold:

$$(\mathbf{a} \cdot \mathbf{A}) \cdot \mathbf{b} = \mathbf{b} \cdot (\mathbf{A} \cdot \mathbf{a}) = \sum_i \sum_j a_i A_{ij} b_j.$$

so that there is no ambigity in writing $\mathbf{a} \cdot \mathbf{A} \cdot \mathbf{b}$.

Differential operators

The expression in what follows are valid in a rectilinear coordinate system, where the basis vectors $\mathbf{e}_i$ are independent of position, and can be treated as constant. The gradient

is defined for tensors of order $p \in \{0, 1\}$, yielding a tensor of order $p + 1$:

$$\nabla f = \frac{\partial f}{\partial x_1}\mathbf{e}_1 + \frac{\partial f}{\partial x_2}\mathbf{e}_2 + \frac{\partial f}{\partial x_3}\mathbf{e}_3 = \sum_i \frac{\partial f}{\partial x_i}\mathbf{e}_i$$

$$\nabla \mathbf{v} = \sum_i \sum_j \frac{\partial v_i}{\partial x_j}\mathbf{e}_i \otimes \mathbf{e}_j = \begin{bmatrix} \partial v_1/\partial x_1 & \partial v_1/\partial x_2 & \partial v_1/\partial x_3 \\ \partial v_2/\partial x_1 & \partial v_2/\partial x_2 & \partial v_2/\partial x_3 \\ \partial v_3/\partial x_1 & \partial v_3/\partial x_2 & \partial v_3/\partial x_3 \end{bmatrix}.$$

The divergence is defined for tensors of order $p \in \{1, 2\}$ and yields a tensor of order $p - 1$:

$$\operatorname{div} \mathbf{v} = \frac{\partial v_1}{\partial x_1} + \frac{\partial v_2}{\partial x_2} + \frac{\partial v_3}{\partial x_3} = \sum_i \frac{\partial v_i}{\partial x_i}$$

$$\operatorname{div} \mathbf{A} = \sum_i \sum_j \frac{\partial A_{ij}}{\partial x_i}\mathbf{e}_j$$

And finally the Laplacian is defined for tenors of order $p \in \{0, 1, 2\}$ and yields again a tensor of order p:

$$\Delta f = \sum_i \frac{\partial^2 f}{\partial x_i^2}$$

$$\Delta \mathbf{v} = \mathbf{e}_1 \Delta v_1 + \mathbf{e}_2 \Delta v_2 + \mathbf{e}_3 \Delta v_3 = \sum_i \sum_j \frac{\partial^2 v_j}{\partial x_i^2}\mathbf{e}_j$$

B. Fundamental concepts of continuum mechanics

This a is brief summary of concepts used throughout the thesis, loosely based on [25].

B.1. Definitions

A fundamental concept used for modeling fluids is that of a *control volume*.

Definition 9 (Control volume)**.** *For the purpose of our a discussion, a control volume is a bounded, simply connected subset of* $\mathbb{R}^3$ *which has a smooth surface (also referred to as control surface) as its boundary.*

We will denote the control volume by $V(t)$ and its surface by $S(t)$ to make it clear that a control volume is allowed to move and change its shape in time. The velocity of a point on the surface will be denoted by $\mathbf{v}_S$, whereas the velocity of the fluid at an arbitrary point by $\mathbf{v}$. The fluid velocity relative to the control surface at a given point on the surface may thus be expressed as $\mathbf{v} - \mathbf{v}_S$.

Definition 10 (Material volume)**.** *A control volume is a material volume if the velocity of its surface,* $\mathbf{v}_S$ *always equals the local fluid velocity, that is,* $\mathbf{v}_S = \mathbf{v}$.

B.2. Conserved quantities

The total mass in a control volume can be expressed by the volume integral $\int_{V(t)} \rho \, dV$ and its conservation by

$$\frac{d}{dt}\int_{V(t)} \rho \, dV = \underbrace{\int_{S(t)} \rho(\mathbf{v}_S - \mathbf{v}) \cdot \widehat{\boldsymbol{n}} \, dS}_{\text{inflow by convection}} + \underbrace{\int_{V(t)} R_\rho \, dV}_{\text{rate of formation}} \tag{B.1}$$

At the same time, we have by the Leibniz rule:

$$\frac{d}{dt}\int_{V(t)} \rho \, dV = \int_{V(t)} \frac{\partial \rho}{\partial t} \, dV + \int_{S(t)} \rho \mathbf{v}_S \cdot \widehat{\boldsymbol{n}} \, dS \tag{B.2}$$

Combining these two equations, the terms containing $\mathbf{v}_S$ cancel and we are left with:

$$\int_{V(t)} \frac{\partial \rho}{\partial t} \, dV + \int_{S(t)} \rho \mathbf{v} \cdot \widehat{\boldsymbol{n}} \, dS - \int_{V(t)} R_\rho \, dV = 0. \tag{B.3}$$

Applying the divergence theorem yields

$$\int_{V(t)} \left(\frac{\partial \rho}{\partial t} + \rho \operatorname{div} \mathbf{v} \right) dV = 0 \tag{B.4}$$

and since both the control volume and its surface were arbitrary (note that even their time dependence was allowed), the integrands must be equal everywhere. We thus get the *continuity equation*:

$$\frac{\partial \rho}{\partial t} + \rho \operatorname{div} \mathbf{v} = R_\rho \tag{B.5}$$

Analogously, the total momentum in a control volume is $\int_{V(t)} (\rho \mathbf{v})\, dV$. The equations are the same as in the case of mass, except now the source terms are the forces. Again, combining the conservation equation:

$$\underbrace{\frac{d}{dt} \int_{V(t)} (\rho \mathbf{v})\, dV}_{\text{rate of change of momentum}} = \underbrace{\int_{S(t)} (\rho \mathbf{v})(\mathbf{v}_S - \mathbf{v}) \cdot \widehat{\boldsymbol{n}}\, dS}_{\text{inflow of momentum}} + \underbrace{\int_{V(t)} \mathbf{f}_V\, dV}_{\text{volume forces}} + \underbrace{\int_{S(t)} \mathbf{f}_S\, dS}_{\text{surface forces}} \tag{B.6}$$

with the Leibniz rule:

$$\frac{d}{dt} \int_{V(t)} (\rho \mathbf{v})\, dV = \int_{V(t)} \frac{\partial (\rho \mathbf{v})}{\partial t}\, dV + \int_{S(t)} (\rho \mathbf{v}) \mathbf{v}_S \cdot \widehat{\boldsymbol{n}}\, dS \tag{B.7}$$

we get

$$\int_{V(t)} \frac{\partial (\rho \mathbf{v})}{\partial t}\, dV + \int_{S(t)} (\rho \mathbf{v}) \mathbf{v} \cdot \widehat{\boldsymbol{n}}\, dS = \int_{V(t)} \mathbf{f}_V\, dV + \int_{S(t)} \mathbf{f}_S\, dS. \tag{B.8}$$

We again rewrite the LHS, this time using the divergence theorem for tensors to yield

$$\int_{V(t)} \frac{\partial (\rho \mathbf{v})}{\partial t} + \operatorname{div}(\rho \mathbf{v} \otimes \mathbf{v})\, dV \tag{B.9}$$

we finally obtain

$$\int_{V(t)} \frac{\partial}{\partial t}(\rho \mathbf{v}) + \operatorname{div}(\rho \mathbf{v} \otimes \mathbf{v})\, dV = \int_{V(t)} \mathbf{f}_V\, dV + \int_{S(t)} \mathbf{f}_S\, dS. \tag{B.10}$$

Combining the steps (B.7) and (B.9) to yield

$$\frac{d}{dt} \int_{V(t)} (\rho \mathbf{v})\, dV = \int_{V(t)} \frac{\partial}{\partial t}(\rho \mathbf{v}) + \operatorname{div}(\rho \mathbf{v} \otimes \mathbf{v})\, dV \tag{B.11}$$

is referred to as the *Reynold's transport theorem.*

Cited literature

[1] Donald A. Drew. Averaged field equations for two-phase media. *Studies in Applied Mathematics*, 50(2):133–166, 1971.

[2] Donald A. Drew. Mathematical modeling of two-phase flow. *Annual Review of Fluid Mechanics*, 15:261–291, 1983.

[3] M.A. Delele, F. Weigler, G. Franke, and J. Mellmann. Studying the solids and fluid flow behavior in rotary drums based on a multiphase cfd model. *Powder Technology*, 292:260–271, 2016.

[4] F. Hager, C. Kloss, and C. Pirker, S. Goniva. Parallel resolved open source cfd-dem: Method, validation and application. *Journal of Computational Multiphase Flows*, 6, 2014.

[5] L. Schwartz. *Mathematics for the Physical Sciences.* Adiwes international series in mathematics. Hermann, 1966.

[6] Francois Treves. *Topological Vector Spaces, Distributions and Kernels: Pure and Applied Mathematics, Vol. 25.* Academic Press, 1967.

[7] L.C. Evans. *Partial Differential Equations.* Graduate studies in mathematics. American Mathematical Society, 2010.

[8] Barbara Burke Hubbard John H. Hubbard. *Vector Calculus, Linear Algebra, and Differential Forms: A Unified Approach.* Matrix Editions, 2007.

[9] Z. Y. Zhou, S. B. Kuang, K. W. Chu, and A. B. Yu. Discrete particle simulation of particle–fluid flow: model formulations and their applicability. *Journal of Fluid Mechanics*, 661:482–510, 2010.

[10] Ariane Bérard, Gregory S. Patience, and Bruno Blais. Experimental methods in chemical engineering: Unresolved cfd-dem. *The Canadian Journal of Chemical Engineering*, 98(2):424–440, 2020.

[11] João A. A. Oliveira Jr. Clarissa B. Fonte and Lucilla C. de Almeida. Dem-cfd coupling: Mathematical modelling and case studies using rocky-dem® and ansys fluent®. *Eleventh International Conference on CFD in the Minerals and Process Industries*, 2015.

[12] Jingyuan Zhang, Tian Li, Henrik Ström, Boyao Wang, and Terese Løvås. A novel coupling method for unresolved cfd-dem modeling. *International Journal of Heat and Mass Transfer*, 203:123817, 2023.

[13] Frank M. White. *Fluid Mechanics*. McGraw-Hill Education, 2011.

[14] Lu Huilin and Dimitri Gidaspow. Hydrodynamics of binary fluidization in a riser: Cfd simulation using two granular temperatures. *Chemical Engineering Science*, 58(16):3777–3792, 2003.

[15] ANSYS, Inc. *ANSYS Rocky User's Guide*, 2023. Version 2023 R1.

[16] F. Moukalled, L. Mangani, and M. Darwish. *The Finite Volume Method in Computational Fluid Dynamics: An Advanced Introduction with OpenFOAM® and Matlab*. Springer International Publishing, 2016.

[17] J.S. Marshall and K. Sala. Comparison of methods for computing the concentration field of a particulate flow. *International Journal of Multiphase Flow*, 56:4–14, 2013.

[18] András Bezdek and Włodzimierz Kuperberg. Dense packing of space with various convex solids. *Geometry—Intuitive, Discrete, and Convex: A Tribute to László Fejes Tóth*, pages 65–90, 2013.

[19] Lloyd N. Trefethen and David Bau III. *Numerical Linear Algebra*. SIAM, Philadelphia, PA, 1997.

[20] S Armfield and R Street. The fractional-step method for the navier–stokes equations on staggered grids: The accuracy of three variations. *Journal of Computational Physics*, 153(2):660–665, 1999.

[21] ANSYS, Inc. *ANSYS Fluent User's Guide*, 2023. Version 2023 R1.

[22] S. Pirker, D. Kahrimanovic, and C. Goniva. Improving the applicability of discrete phase simulations by smoothening their exchange fields. *Applied Mathematical Modelling*, 35(5):2479–2488, 2011.

[23] Daniel A. Clarke, Andrew J. Sederman, Lynn F. Gladden, and Daniel J. Holland. Investigation of void fraction schemes for use with cfd-dem simulations of fluidized beds. *Industrial & Engineering Chemistry Research*, 57(8):3002–3013, 2018.

[24] Hermann Schlichting and Klaus Gersten. *Boundary-Layer Theory*. Springer, 2017.

[25] W.M. Deen. *Analysis of Transport Phenomena*. OUP USA, 2012.